AD NUMBER

ADB015617

NEW LIMITATION CHANGE

TO

Approved for public release, distribution unlimited

FROM

Distribution authorized to U.S. Gov't. agencies only; Administrative/Operational use; Dec 1976. Other requests shall be referred to Naval Weapons Center, China Lake, CA 93555-0000.

AUTHORITY

USNWC notice 23 Jan 1979

NWC TP 5892

Development of Optimum Theoretical Warhead Design Criteria

by
T. Zulkowski
Propulsion Development Department

DECEMBER 1976

Naval Weapons Center
CHINA LAKE, CALIFORNIA 93555

Naval Weapons Center

AN ACTIVITY OF THE NAVAL MATERIAL COMMAND

R. G. Freeman, III, RAdm., USN . . . . . Commander

G. L. Hollingsworth . . . . . Technical Director

FOREWORD

This report describes an analytical study conducted during the period January through May 1976, to develop optimum theoretical warhead design criteria. This effort was funded by the Naval Air Systems Command under Program Element 62332N, Subproject WF32-352-502.

R.G.S. Sewell has reviewed this report for technical accuracy.

Released by
G. W. LEONARD, *Head*
Propulsion Development Department
1 August 1976

Under authority of
G. L. HOLLINGSWORTH
Technical Director

NWC Technical Publication 5892

Published by . . . . . Technical Information Department
Collation . . . . . Cover, 19 leaves
First printing . . . . . 185 unnumbered copies

UNCLASSIFIED

SECURITY CLASSIFICATION OF THIS PAGE *(When Data Entered)*

REPORT DOCUMENTATION PAGE

READ INSTRUCTIONS BEFORE COMPLETING FORM

1. REPORT NUMBER: NWC-TP-5892	2. GOVT ACCESSION NO.
3. RECIPIENT'S CATALOG NUMBER	
4. TITLE *(and Subtitle)*: DEVELOPMENT OF OPTIMUM THEORETICAL WARHEAD DESIGN CRITERIA	5. TYPE OF REPORT & PERIOD COVERED: Final report January-May 1976
	6. PERFORMING ORG. REPORT NUMBER
7. AUTHOR(s): T. Zulkoski	8. CONTRACT OR GRANT NUMBER(s)
9. PERFORMING ORGANIZATION NAME AND ADDRESS: Naval Weapons Center, China Lake, California 93555	10. PROGRAM ELEMENT, PROJECT, TASK AREA & WORK UNIT NUMBERS: Program Element 62332N, Subproject WF32-352-502
11. CONTROLLING OFFICE NAME AND ADDRESS: Naval Air Systems Command, Washington, DC 20360	12. REPORT DATE: December 1976
	13. NUMBER OF PAGES: 36
14. MONITORING AGENCY NAME & ADDRESS *(if different from Controlling Office)*	15. SECURITY CLASS. *(of this report)*: UNCLASSIFIED
	15a. DECLASSIFICATION/DOWNGRADING SCHEDULE

16. DISTRIBUTION STATEMENT *(of this Report)*

Distribution limited to U.S. Government agencies only; test and evaluation; 30 September 1976. Other requests for this document must be referred to the Naval Weapons Center.

17. DISTRIBUTION STATEMENT *(of the abstract entered in Block 20, if different from Report)*

18. SUPPLEMENTARY NOTES

19. KEY WORDS *(Continue on reverse side if necessary and identify by block number)*

Warhead Design
Fragment Kinetic Energy
Solid Cylinder
End Effects

20. ABSTRACT *(Continue on reverse side if necessary and identify by block number)*

See reverse side of this form.

DD FORM 1 JAN 73 1473 EDITION OF 1 NOV 65 IS OBSOLETE
S/N 0102-014-6601

UNCLASSIFIED

SECURITY CLASSIFICATION OF THIS PAGE *(When Data Entered)*

(U) *Development of Optimum Theoretical Warhead Design Criteria*, by T. Zulkoski. China Lake, Calif., Naval Weapons Center, December 1976. 36 pp. (NWC TP 5892, publication UNCLASSIFIED.)

(U) A study was conducted to develop optimum theoretical warhead design criteria. Weight, diameter and length constraints were considered based on a solid cylinder with no end confinement. End effects were also considered and treated using correction factors in the form of exponential functions of length-to-diameter ratios. Using these parameters, three general qualitative conclusions were drawn: (1) the greater the warhead length, the greater its initial fragment kinetic energy, (2) the mathematical models developed indicate that the optimum charge-to-metal mass ratio (C/M) is greater than 1.4 and that a decreased length-to-diameter ratio results in higher optimum C/Ms; and (3) optimum warhead case material, from the standpoint of initial fragment kinetic energy, is a function of warhead weight, length and diameter.

CONTENTS

The following conversion factors are provided to allow the reader to convert standard units used in this report to metric equivalents:

To convert from	to	Multiply by
inch	meter	0.0254
pound-mass	kilogram	0.4535
pound-mass/inch^3	kilogram/meter^3	27679.9
slug	kilogram	14.5939

INTRODUCTION

An optimum theoretical warhead design is needed primarily during the early stages of warhead design. Systems analysts also need such information when they are attempting to evaluate systems performance in early systems synthesis. In recent years, the primary parameter for determining optimum warhead designs has been an energy criteria; initial fragment kinetic energy being one of the first factors of concern.

The warhead environment is quite variable and all the conditions imposed have an effect on the energy characteristics of the warhead. A study by R.G.S. Sewell considered several of these conditions in determining an optimum charge-to-metal ratio for both weight and volume contrained warheads.[1] In making the determinations of optimum charge-to-metal ratios, Sewell used Gurney formulas to evaluate initial fragment velocities and kinetic energies and, for the sake of simplicity, accepted the assumptions implicit in these formulas. The most significant of these assumptions relative to practical warhead designs is that there are no end effects to modify the initial fragment velocity and, hence, no effect on initial fragment kinetic energy. However, past experience with cased cylindrical explosive charges has shown that this is not the case and that velocity variations at the ends of the warhead are significant due to these end effects. Thus, to determine the initial fragment kinetic energy, these end effects must be included in the warhead design consideration.

METHOD

The study effort reported herein is basically a continuation and expansion of the work done by Sewell (see footnote 1). His work served both as a basis and starting point for this effort.

This study, as did Sewell's, considers weight constraints imposed on the warhead. But, instead of a volume constraint being imposed, separate considerations of both diameter and length are included. To this has been added the consideration of end effects; these appear as correction factors in the form of exponential functions of length-to-diameter ratios. Although only kinetic energy ($1/2\ mv^2$) is of concern here, the same general procedures can be used on other optimization criteria such as momentum (mv) or any other parameter involving mass and velocity, e.g., $mv^{3/2}$. Additionally, only a solid cylinder with no end confinement is considered in this study. Any other configuration, such as a hollow cylinder or use of appreciable end confinement, would require new correction factors since the modified end effects for each configuration would have to be determined.

[1] Naval Ordnance Test Station. *Fixed-Weight and Volume Constraints on Optimum Charge-to-Metal Ratios in Warhead Design*, by R.G.S. Sewell. China Lake, Calif., NOTS, March 1964. (NOTS TP 3430, publication UNCLASSIFIED.)

This is a relatively simple method. However, it is highly dependent on the quality of the input data. Because the data employed were not generated under this study effort, appropriate references for these data were used to generate correction factors for the velocity as a function of length-to-diameter ratios (L/D) at the initiated and uninitiated ends of a cylindrical warhead. These velocity correction factors were then combined with the Gurney equation for a solid cylinder and included as a part of the incremental energy equation. Integration of that equation resulted in the total initial fragment kinetic energy for a given set of input parameters. Depending upon which velocity correction factors were used, three different initiation schemes could be considered, as shown in Figure 1. Single-point, one end, center initiation (Figure 1a) served as the baseline, while the center initiation (Figure 1b) and simultaneous dual-end center initiation (Figure 1c) schemes were modeled by choosing the appropriate combinations of correction factors.

VELOCITY CORRECTION FACTORS

Derivation of the velocity correction factors is the first step. Because the release effects are different on each end of a single end initiated cylinder, each end of the cylinder will be treated separately. Mathematically this assumes that the entire correction factor is the product of two independent functions of length, i.e.,

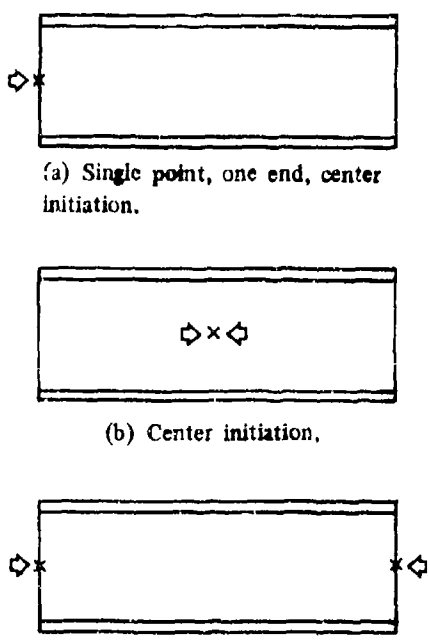

(a) Single point, one end, center initiation.

(b) Center initiation.

(c) Simultaneous dual end center point initiation.

FIGURE 1. Initiation Schemes.

$$C_f = F(\ell/d) \cdot G(\ell/d) \quad (1)$$

where

C_f is the velocity correction factor
ℓ/d is the position in length-to-diameter ratio of explosive charges on the charge
$F(\ell/d)$ is the correction at the initiated end
$G(\ell/d)$ is the correction at the uninitiated end

The problem, then, becomes one of determining $F(\ell/d)$ and $G(\ell/d)$ for the cylinders.

Review of available literature would indicate only very limited work has been done in this area. A plot of correction factor versus length in L/D (Figure 2) for single point end initiation was found.[2] These data were used because of their convenient form and availability. It was assumed that the correction factor applied to initial velocity at various points on the cylinder rather than average velocity of the overall cylinder and that the charge mass to metal mass ratio was sufficiently high that the metal case thickness was small compared to the metal case outside diameter.

A modified least squares fit was done to the curve to put the data in the form of an equation. The result is also plotted in Figure 2. The form of equation used as a correction factor is:

$$F(\ell/d) = 1 - e^{A(\ell/d)} \quad (2)$$

where

$F(\ell/d)$ = correction factor
ℓ/d = position on the case in terms of length-to-diameter ratio of the explosive charge
A = constant = -2.3617

Once the correction factor, $F(\ell/d)$, has been determined, it becomes necessary to determine the correction factor for the uninitiated end, $G(\ell/d)$. The Ballistics Research Laboratories (BRL) had published data[3] which we employed for this purpose. For future simplicity, we will say that $G(\ell/d) = G(x)$, where $x = X(\ell/d)$, x is the distance from the uninitiated end. Introducing this change of variable will make the processing of the BRL data much easier. A least squares fit of the data for several different exponential equations resulted in

[2] FMC Corporation, *The Elusive $\sqrt{2E}$*, by Donald R. Kennedy, Defense Technology Laboratories, Santa Clara, Calif., 22 April 1969. (Publication UNCLASSIFIED.)

[3] American Defense Preparedness Association, *Proceedings of the First International Symposium on Ballistics*, 13-15 November 1974, "Calculation of Fragment Velocities From Fragmentation Munitions," by R. R. Karpp and W. W. Predebon, Ballistics Research Laboratories (publication UNCLASSIFIED.)

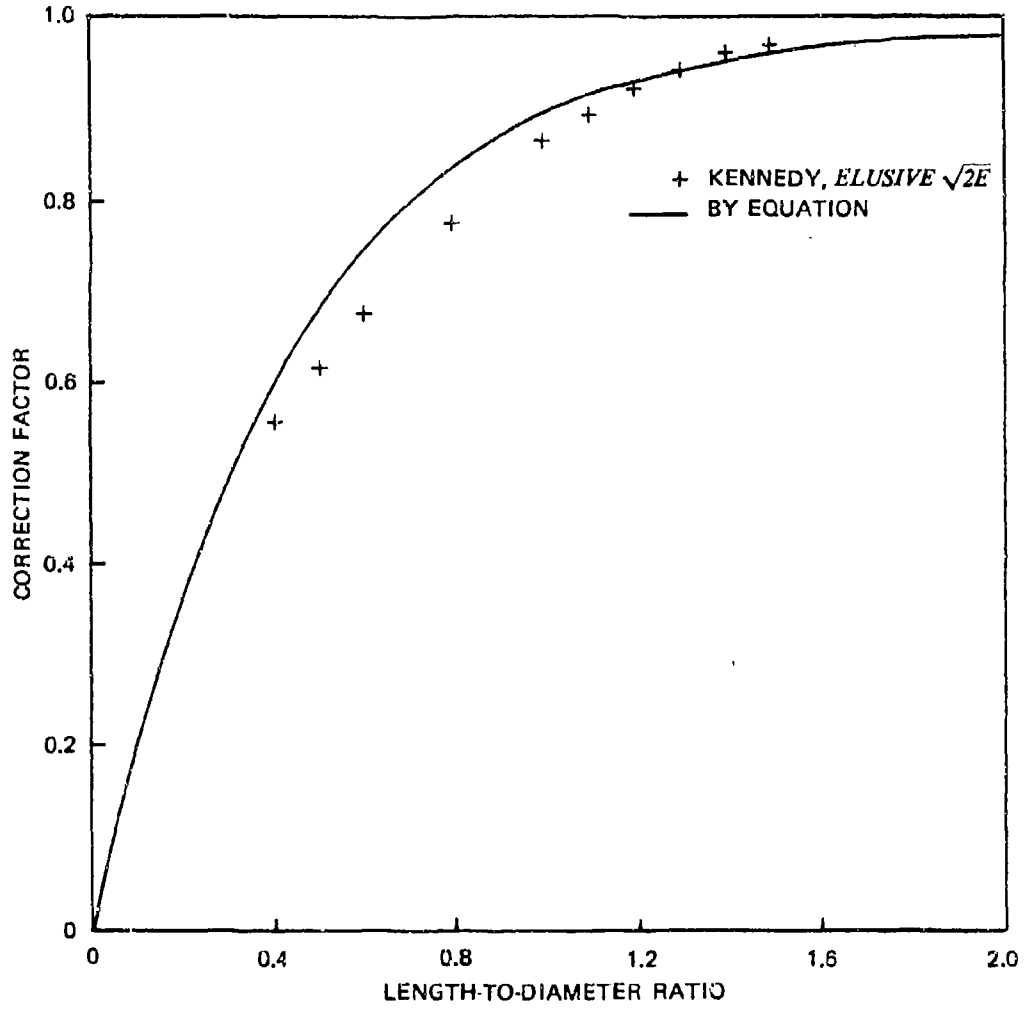

FIGURE 2. Correction Factor Comparison, F(ℓ/d).

$$G(x) = 1 - Be^{Cx} \tag{3}$$

where

B = constant = 0.28806
C = constant = -4.603
x = distance in charge diameters from uninitiated end

Now x can be converted back to a function of ℓ/d such that

$$x = X(\ell/d) = (L - \ell)/d \tag{4}$$

which simply places the position of the point of interest relative to the initiation end.

The form of G(x) was selected on the basis of the best correlation coefficient resulting from the least squares fit. The total correction factor for velocity as a function of position in explosive charge diameters is now

$$C_f = (1 - e^{-2.3617\ell/d})(1 - 0.28806e^{-4.603(L-\ell)/d}) \quad (5)$$

Multiplying this and the Gurney equation should provide a reasonable velocity prediction along the length of a solid cylindrical, metal encased, explosive charge which has been point initiated on one end at the center.

To be completely rigorous, it should be pointed out that Equation 5 is a correction factor for fragment speed. It cannot be used for velocity since velocity is a vector quantity and speed is only the magnitude and says nothing about direction of fragments.

OTHER INITIATION TECHNIQUES

By combining $F(\ell/d)$ and $G(\ell/d)$ in two other ways with small changes in the variable, the initiation methods shown in Figures 1b and 1c can be approximated. The rationale and correction factors are presented in this section.

In the case of center point initiation, as shown in Figure 1b, we find that the release effects at either end of the charge are identical. In addition, they are the same as the uninitiated end of the single end initiated charge. This means that the end correction factor for an uninitiated end can be utilized for both ends if an appropriate change is made in the form of the equation. This change allows treating the velocity from a reference end corresponding to the initiated end in the first case, i.e., $\ell/d = 0$. Thus, for this end of the charge,

$$G(\ell/d) = 1 \quad 0.28806e^{-4.603\ell/d} \quad (6)$$

while on the other end, where $\ell/d = L/D$, the correction factor is simply Equation 3. Hence, this correction factor is

$$C_f = (1 - 0.28806e^{-4.603\ell/d})(1 - 0.28806e^{-4.603(L-\ell/d)}) \quad (7)$$

The center region of the charge for this configuration is assumed, in this model, to be unaffected by the initiation point location. This is a reasonable assumption as long as only the magnitude of the velocity is of interest. It is not correct if direction is of concern since an appropriate treatment of the vector problem must also be made. However, our concern is with magnitude only, thus, we need only justify that the velocity magnitude is unchanged. It was determined,* from both theoretical and experimental information, that normal impact of the detonation waves

* Personal discussions between the author and Mr. R.G.S. Sewell of NWC.

under the conditions existing in this problem do not change the maximum or initial velocity; only the acceleration profile of the fragmentation is modified. This is because the actual impulse remains about constant in this region for either normal or sweeping detonation waves. The higher pressures from a normally impacting detonation wave are also of shorter duration. Conversely, longer durations and lower pressures are characteristic of a sweeping detonation wave: hence, the resulting change in acceleration profile with the same limiting "velocity".

In the case of simultaneous dual end initiation, as shown in Figure 1c, both ends are initiated. Utilizing the same considerations as before, we find the correction factor at the reference end to be Equation 2 only. Now using x in place of ℓ/d for the opposite end, and making appropriate substitutions, the correction factor becomes

$$C_f = (1 - e^{-2.3617\ell/d})(1 - e^{-2.3617(L-\ell)/d}) \tag{8}$$

The main assumption in this case is that the center interaction zone, where the detonation waves meet, does not change the velocity magnitude of the fragmentation system. Supporting this assumption is the width of the reaction zone in the explosive; on the order of 0.1-0.2 inch thick. Conversely, limited test data would indicate that, although the explosive interaction zone is very narrow, the effect on fragmentation velocity is significant over a much larger percentage of the warhead length. For our purpose, the assumption will be considered valid. However, this model should be considered, at best, useful only for generation of trends because of the apparent lack of validity of this assumption.

FRAGMENT INITIAL KINETIC ENERGY

There now exist correction factors which, applied to the Gurney equation for a solid cylinder, will predict initial velocities at any point along the length of the cylinder. And this, in turn, can be used to predict fragment initial kinetic energy or potential energy within a solid cylindrical configuration for any of the various initiation systems shown. Figure 3 will be referred to in the following section as an aid in developing the appropriate equations. It consists of a constant diameter (d) explosive charge having length (L) and encased within a constant wall thickness metal sleeve.

The energy of that cylinder can be determined as follows. First, the energy at any point along the cylinder is:

$$dE = \frac{1}{2} dm v^2 \tag{9}$$

where the incremental mass, dm, of the metal case is defined as

$$dm = \rho_m \pi \left(\frac{D^2}{4} - \frac{d^2}{4} \right) d\ell \tag{10}$$

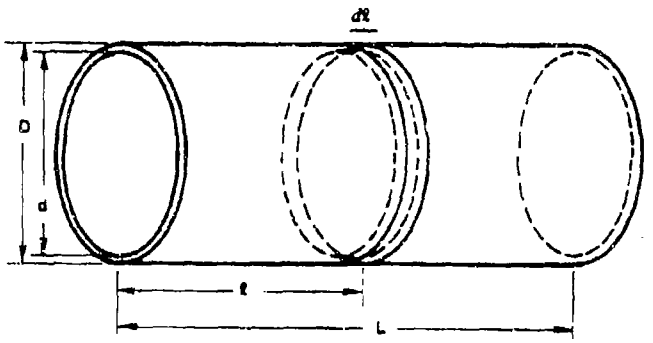

FIGURE 3. Charge Configuration.

where ρ_m = density of the metal case.

Equation 10 can be rewritten in terms of the variable y as follows:

$$dm = \rho_m \pi\left(\frac{D^2}{4} - \frac{d^2}{4}\right)d\ell dy \tag{11}$$

where

$$y = \ell/d$$
$$dy = d\ell/d$$

The initial velocity (v) in Equation 9 requires the application of Equation 5 to the Gurney equation. The velocity equation now becomes:

$$v = (1 - e^{-2.3617y})(1 + 0.28806e^{-4.6033(Y-y)})\alpha\sqrt{\frac{C/M}{1+.5\,C/M}} \tag{12}$$

where

Y = L/d
α = Gurney constant characteristic of the explosive
C/M = ratio of charge mass to metal mass

In order to determine the total initial fragment kinetic energy, E_{TOT}, in the system, Equation 9 must be integrated over the full length of the warhead. Hence,

$$E_{TOT} = \frac{1}{2}\int_0^Y v^2\,\rho_m \pi\left(\frac{D^2}{4} - \frac{d^2}{4}\right)d\ell dy \tag{13}$$

Substituting Equation 12 into Equation 13,

$$\frac{E_{TOT}}{\alpha^2} = \frac{1}{2}\rho_m \pi \left(\frac{D^2}{4} - d^2\right) d\left(\frac{C/M}{1+0.5\,C/M}\right) \int_0^Y [(1 - e^{-2.3617y})$$

$$(1 - 0.28806e^{-4.603(Y-y)})]^2 dy \tag{14}$$

The integral itself is simple but tedious to evaluate. By expanding, integrating term-wise, and reducing to its simplest form, we have the integral

$$\int_0^Y [(1 - e^{-2.3617y})(1 - 0.28806e^{-4.603(Y-y)})]^2 dy = -0.75128 + Y$$

$$+ 1.3367e^{-2.3617Y} - 5.1740e^{-4.603Y} + 4.5918e^{-4.7234Y}$$

$$- 0.00328e^{-9.206Y} \tag{15}$$

The last term is so small that for any practical application it can be ignored. Substituting Equation 15 into Equation 14 for the integral results in

$$\frac{E_{TOT}}{\alpha^2} = \frac{1}{2}\rho_m \pi \left(\frac{D^2}{4} - d^2\right) d\left(\frac{C/M}{1+0.5\,C/M}\right) (-0.75128 + L/d + 1.3367e^{-2.3617L/d}$$

$$- 5.1740e^{-4.603L/d} + 4.5918e^{-4.7234L/d}) \tag{16}$$

One additional algebraic manipulation must be done. That is an expression for the explosive charge diameter in terms of the more commonly specified parameters of weight (W), length (L), and outside diameter (D). Writing the expression for W:

$$W = \pi \left(\frac{D^2}{4} - \frac{d^2}{4}\right) L\rho_m + \pi \frac{d^2}{4} L\rho_e \tag{17}$$

Solving Equation 17 for d:

$$d = \left[\left(\frac{4W}{\pi L} - \rho_m D^2\right)/\left(\rho_m + \rho_e\right)\right]^{1/2} \tag{18}$$

And finally the charge-to-mass (C/M) ratio becomes

$$C/M = [\rho_e \pi L(d^2/A)]/\left[\rho_m \pi L\left(\frac{D^2}{4} - \frac{d^2}{4}\right)\right] \tag{19}$$

or

$$C/M = \frac{\rho_e}{\rho_m} \frac{1}{\frac{D^2}{d^2} - 1}$$

This same procedure can be applied to the other initiation techniques shown in Figure 1 as well. The only changes made will be in the correction factors already developed and discussed, e.g., Equations 7 and 8. Hence, only the integral portion of Equation 14 needs to be redone for th cases considered here. For the center initiation, Figure 1b and Equation 7, the integral becomes

$$\int_0^Y [(1 - 0.28806e^{-4.603y})(1 - 0.28806e^{-4.603(Y-y)})]^2 dy = Y - 0.2503 + (0$$

$$+ 0.1782 + 0.3319Y)e^{-4.603Y} + (0.02077 + 0.00688Y)e^{-9.206Y} \quad (20)$$

Once again the last term is significant only for $Y << 1$; therefore, we can ignore it and substitute Equation 20 for the integral in Equation 14.

$$\frac{E_{TOT}}{\alpha^2} = \frac{1}{2}\rho_m \pi \left(D^2 - \frac{d^2}{4}\right) d\left(\frac{C/M}{1+0.5\,C/M}\right)\left[L/d - 0.2503\right.$$

$$\left. + (0.1782 + 0.3319L/d)e^{-4.603L/d}\right] \quad (21)$$

Using this same procedure for the dual end initiation, the integral in Equation 20 becomes

$$\int_0^Y [(1 - e^{-2.3617y})(1 - e^{-2.3617(Y-y)})]^2 dy$$

$$= Y - 1.27027 + 4Ye^{-2.3617Y} + (Y + 1.27027)e^{-4.7234Y} \quad (22)$$

With this now inserted back into the original equation

$$\frac{E}{\alpha^2} = \frac{1}{2}\rho_m \pi \left(D^2 - \frac{d^2}{4}\right) d\left(\frac{C/M}{1+0.5\,C/M}\right)\left[L/d - 1.27027 + 4\frac{L}{d}e^{-2.3617L/d}\right.$$

$$\left. + (L/d + 1.27027)e^{-4.7234L/d}\right] \quad (23)$$

RESULTS

There now exist three sets of equations which will predict the initial fragment kinetic energy output from a solid cylindrical, metal encased, explosive charge of finite length and having no end confinement. A set of parameterized variables were selected and each set of equations applied. The results are shown in Figures 4 through 21. Figures 4 through 9 are for a single end initiated charge as shown in Figure 1a.

Equations 14, 18, and 19 were used to generate those figures. Similarly, Figures 10 through 15 are for a center initiated cylinder and utilized Equations 18, 19, and 21. Figures 16 through 21 are the maximum energy plots for the parameters considered for each initiation method. The parameters used to generate these figures were: weights ranging from 10 to 30 pounds in 5-pound increments, outside diameter ranging from 5 to 8 inches in 1-inch increments, and $\rho_m = 0.283$ in/lb^3 (i.e., steel). The length in terms of the ratio of length to overall outside diameter was parametrically varied for each pair of the above parameters (see Figures 4-8, 10-14, and 16-20). The peak energy values determined for each set of parameters were then plotted in Figures 9, 15, and 21. As summarized in the preceding graphs, these data indicate the L/D and C/M values for maximum E/α^2 to the nearest 0.025. It can be seen that the optimum C/M increases as L/D decreases and in none of the cases considered did the C/M ever drop to 1.4. Also note that increased L/D with correspondingly decreased diameter results in an increase in energy even though weight and volume constraints remain the same. This is to be expected as the end effects become less of a factor on the total energy consideration for the longer warheads. What is surprising is the degree to which this effect is noticed. In some cases considered, the energy varied by more than an order of magnitude due to a change in diameter of less than a factor of two.

In Figures 22 through 25, the impact of fragment density (ρ_m) on initial fragment kinetic energy is considered. Using different ρ_m values impacts the output energy in a linear fashion, as indicated by Equations 10 and 14, but it also affects the results coming out of Equations 18 and 19. It is interesting to note that the energy for the low L/Ds is highest at the lowest densities while the opposite is true for large L/Ds, i.e., high ρ_m results in higher energy. In effect, there is a L/D region where case density will make little difference in energy as well as L/D regions where it will make a significant difference. This is not surprising since the correction factors used when applying this model to each initiation technique would be expected to produce, qualitatively, such an effect. What is surprising is the apparent effect, quantitatively, at the short L/Ds. It can be seen by looking at Figures 9, 15, and 21 that, for very short L/Ds, the effect is very significant. This leads one to consider that sub-calibers, or diameters smaller than the missile outside diameter, may be a desirable way to design warheads simply to increase L/D ratio and, hence, net total energy. However, the increase in unnecessary weight required to design a sub-caliber warhead must also be considered before making such a decision.

CONCLUSIONS

The considerations and resulting curves presented here may prove useful in the design of guided missile warheads by allowing the designer to define the optimum "initial energy" packaging envelope. They do not, however, consider any of the other factors necessary in the design of a warhead such as fragment size or weight, ejection angle, or any other factors affecting hit probability. Therefore, they do not provide all the necessary information for designing a warhead. Although an attempt was made to

consider different types of initiation methods, the assumptions and approximations used are limited. The least accurate model is that of the simultaneous dual end initiation with the interaction zone in the center. Although the model can be used to generate trends, its accuracy is questionable.

Three general conclusions can be drawn from this effort. First, the greater the warhead length, the greater its initial fragment kinetic energy. Note once again that this says nothing about the distribution of that energy. Second, these mathematical models all indicate that the optimum C/M ratio is greater than 1.4 and that decreased L/D results in higher C/M. Third, the optimum case material, from the standpoint of initial fragment kinetic energy, is a function of warhead weight, length, and diameter. Also, there is no reason to believe that changes in optimization design criteria, e.g., momentum or $mv^{3/2}$, will result in the same designs proving optimum. Indeed, the simple exercise of momentum optimization will show this not to be the case. This report merely exemplifies the procedures necessary to accomplish such optimization whatever the optimization criteria.

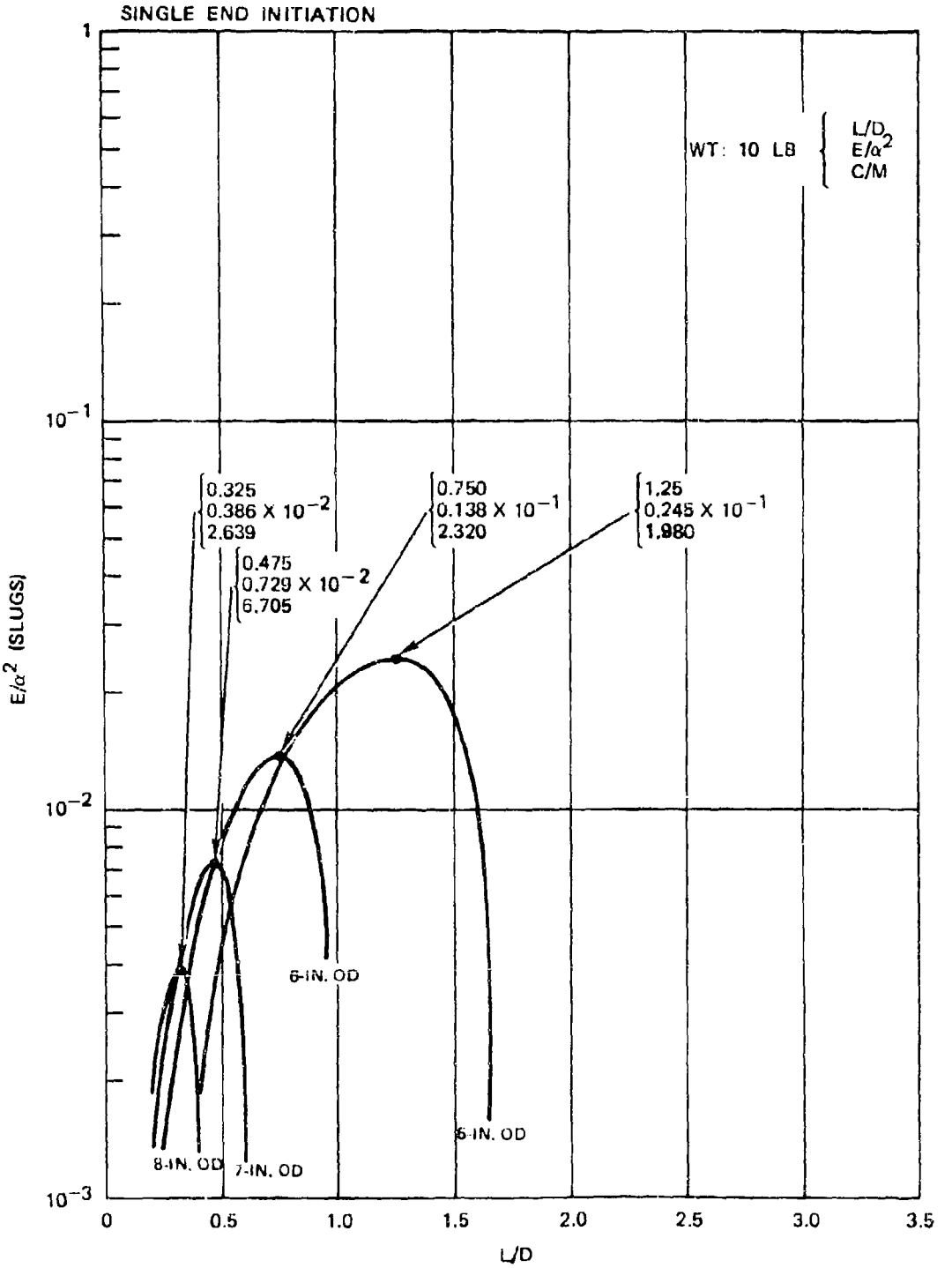

FIGURE 4. Fragment Initial Kinetic Energy Envelopes for Indicated Weight, Single End Initiation.

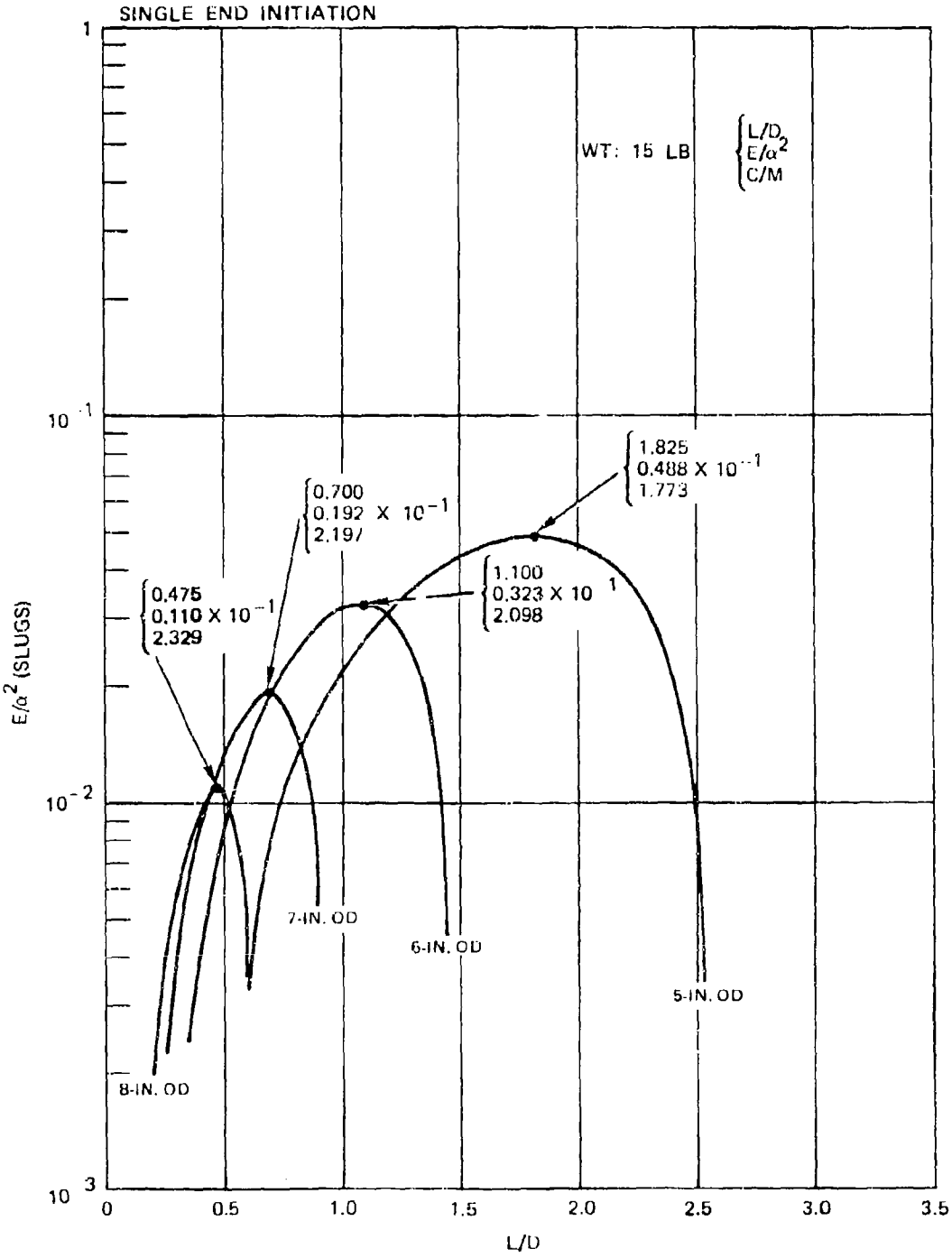

FIGURE 5. Fragment Initial Kinetic Energy Envelopes for Indicated Weight, Single End Initiation.

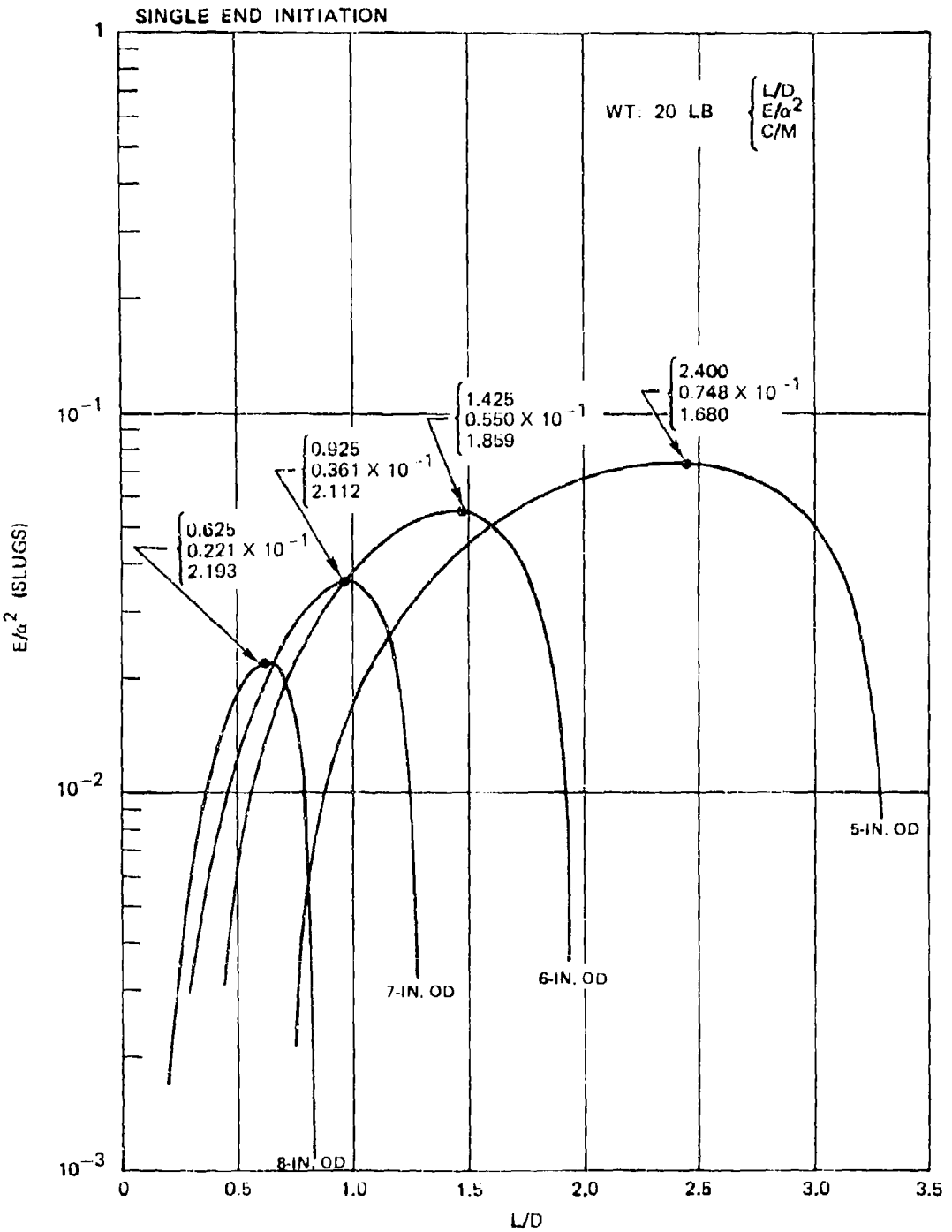

FIGURE 6. Fragment Initial Kinetic Energy Envelopes for Indicated Weight, Single End Initiation.

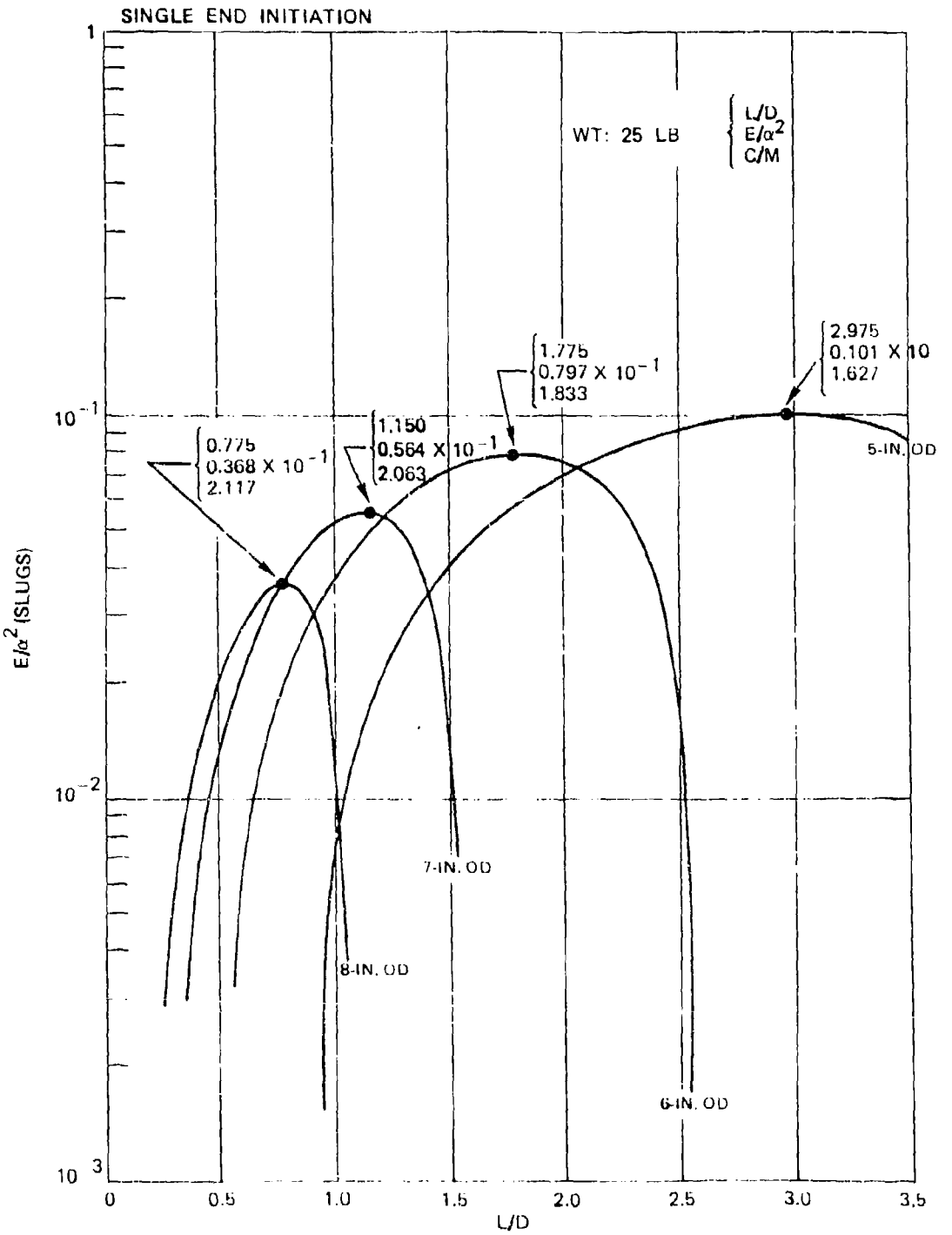

FIGURE 7. Fragment Initial Kinetic Energy Envelopes for Indicated Weight, Single End Initiation.

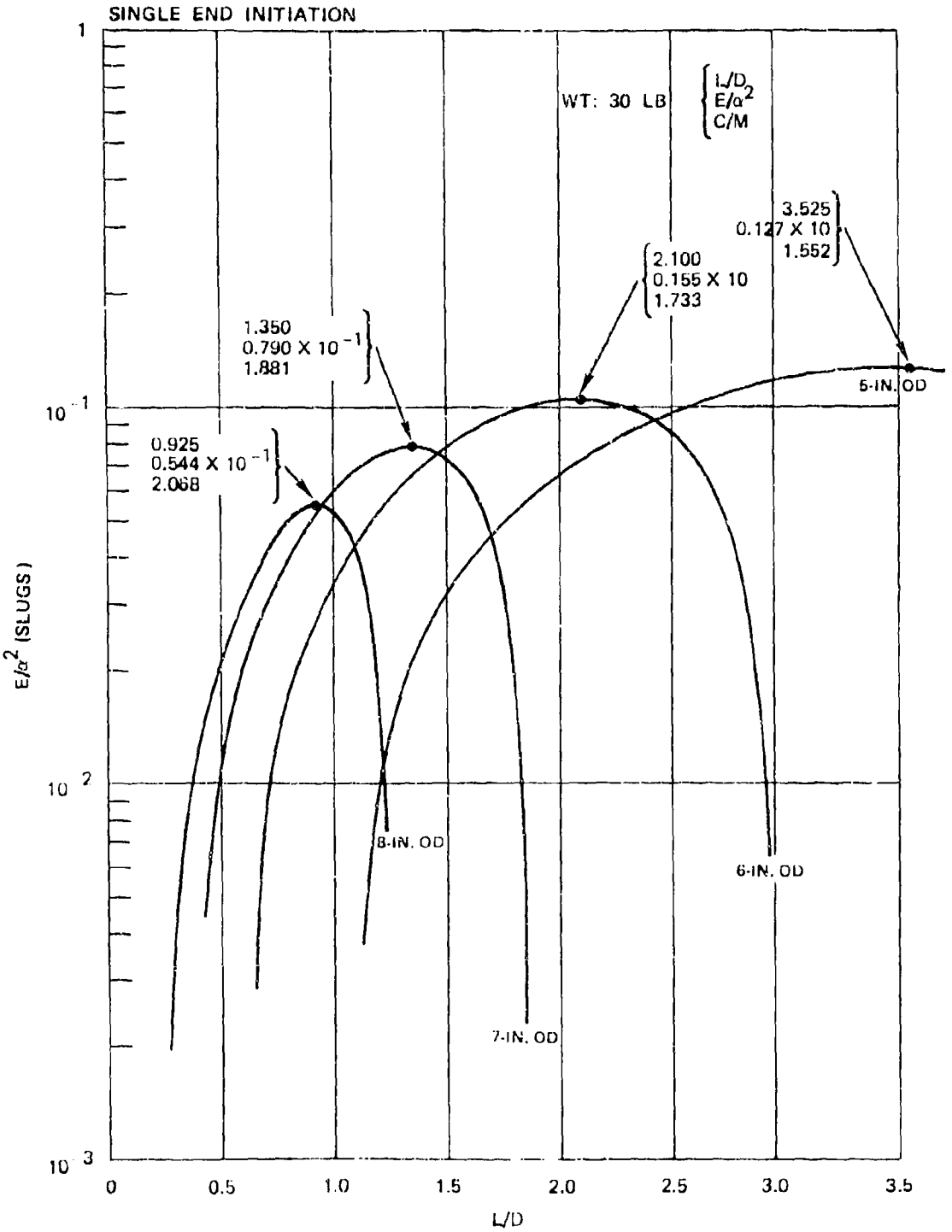

FIGURE 8. Fragment Initial Kinetic Energy Envelopes for Indicated Weight, Single End Initiation.

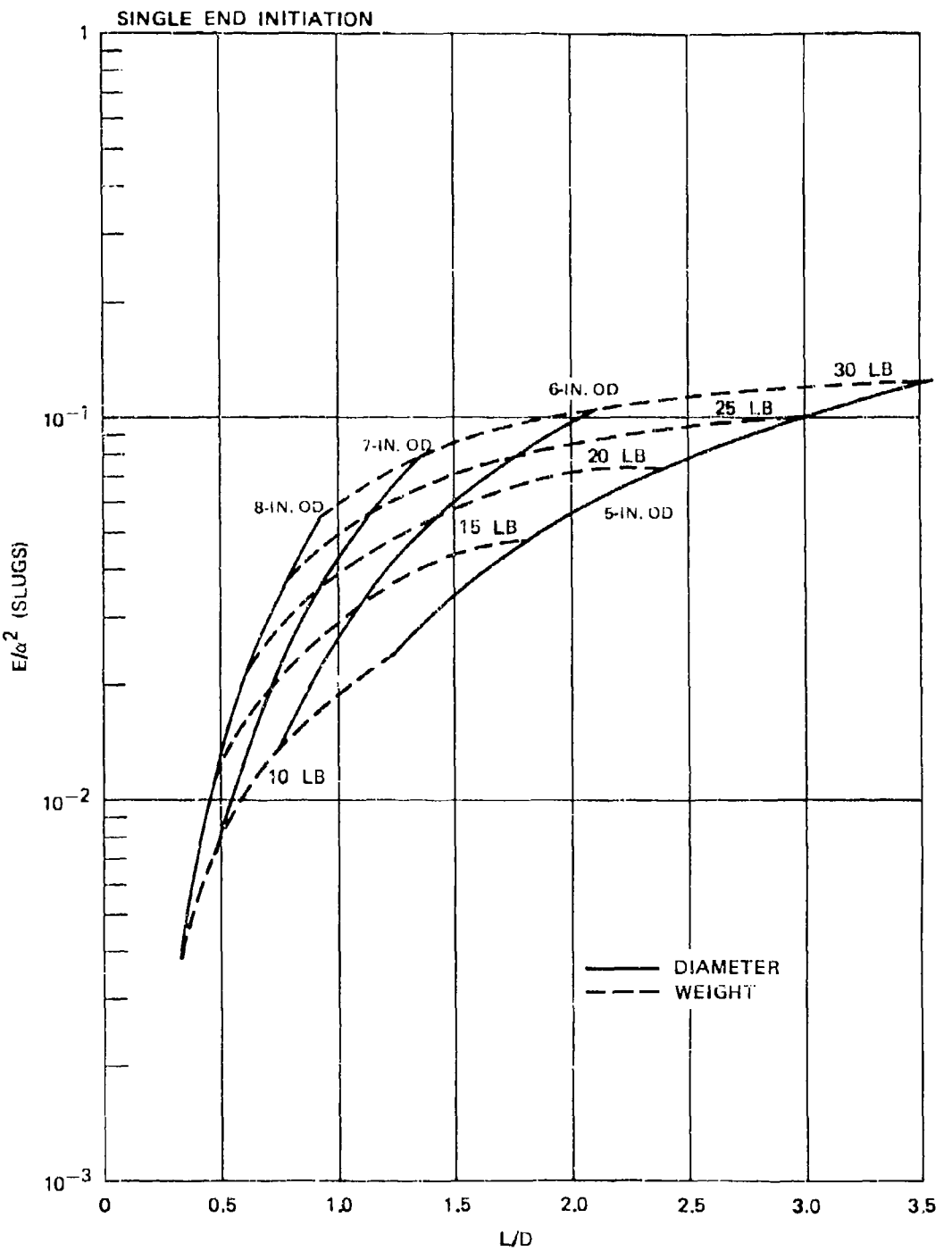

FIGURE 9. Maximum Initial Kinetic Energy Envelopes for Single End Initiation as a Function of Weight and Diameter.

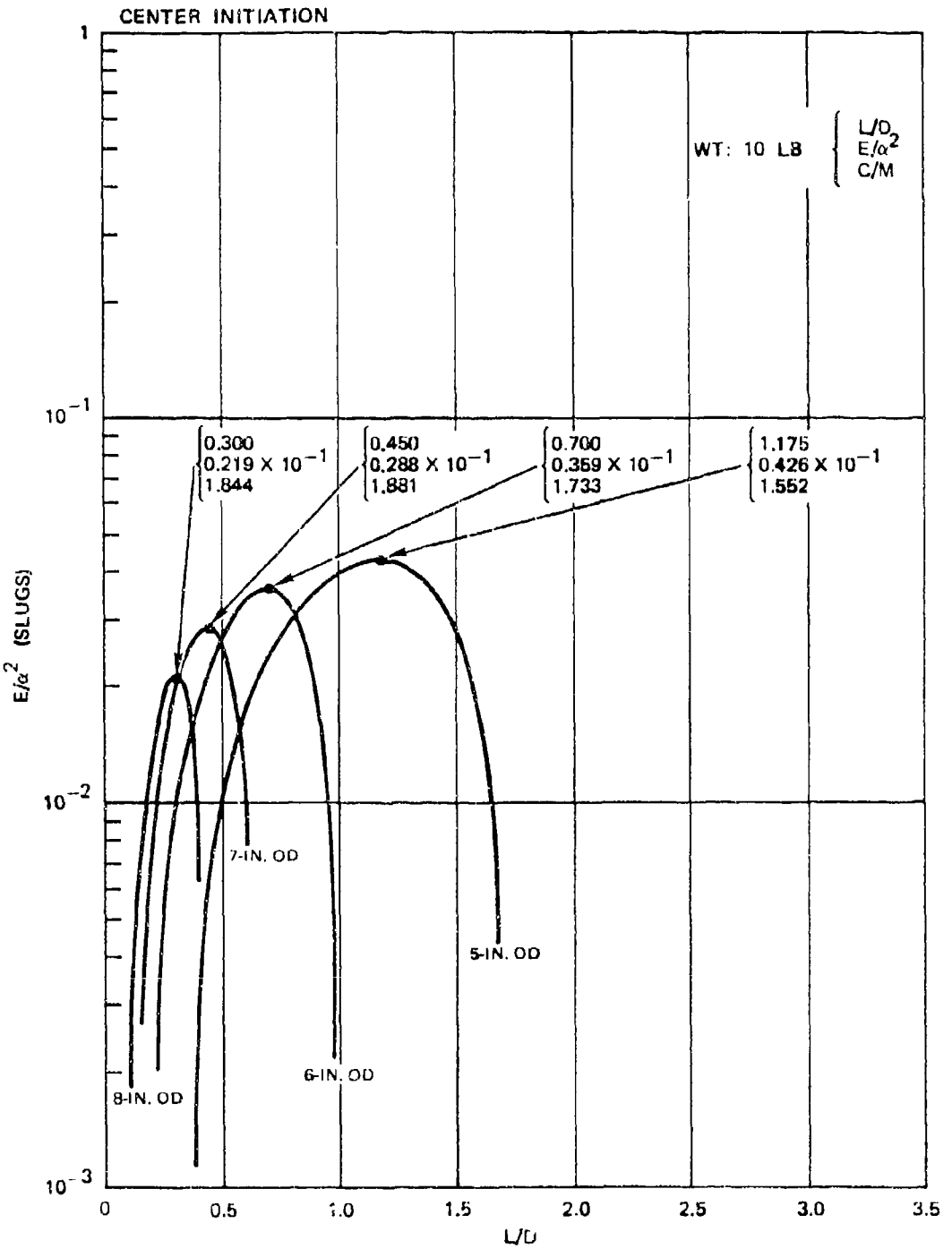

FIGURE 10. Fragment Initial Kinetic Energy Envelopes for Indicated Weight, Center Initiation.

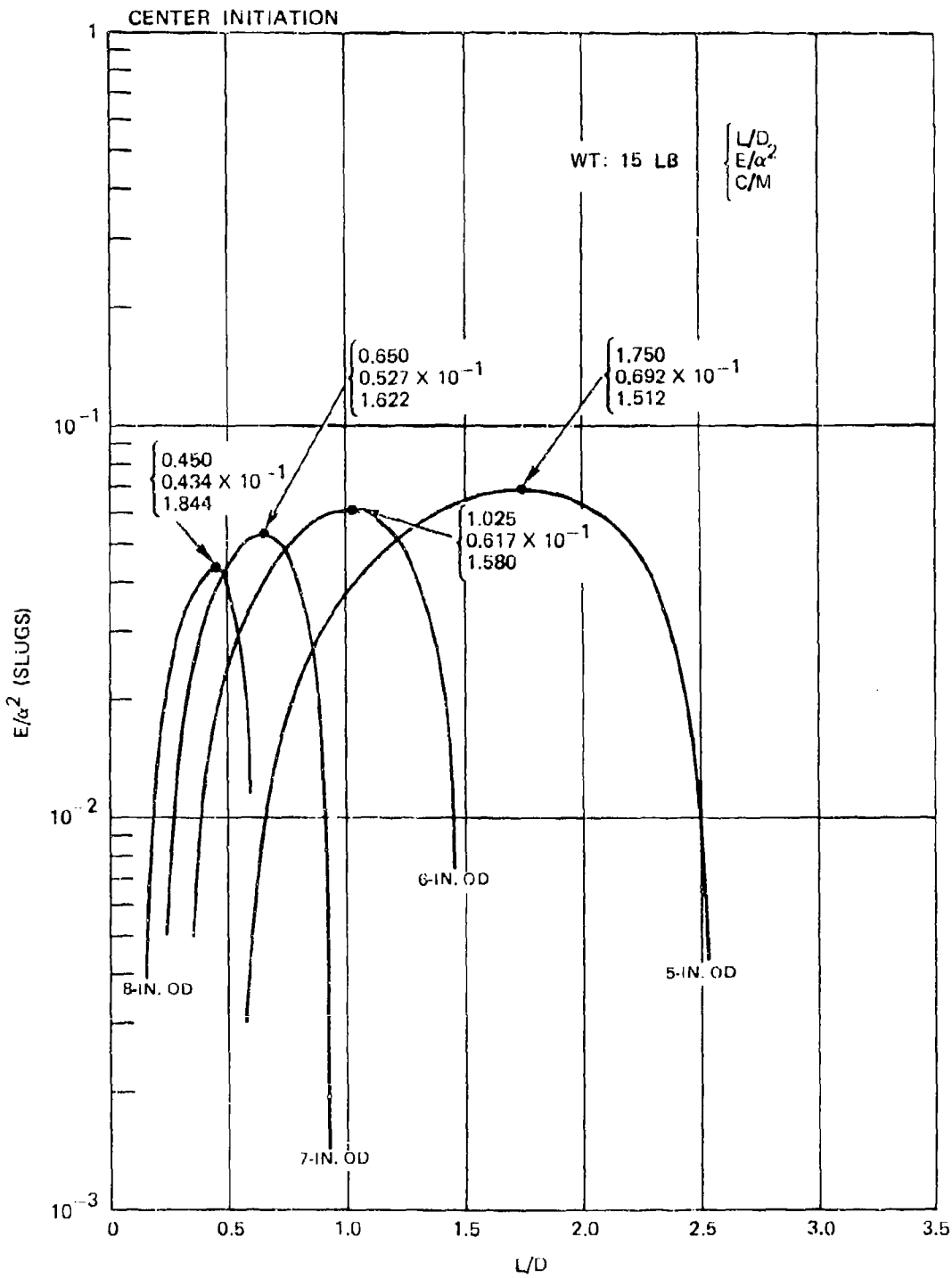

FIGURE 11. Fragment Initial Kinetic Energy Envelopes for Indicated Weight, Center Initiation.

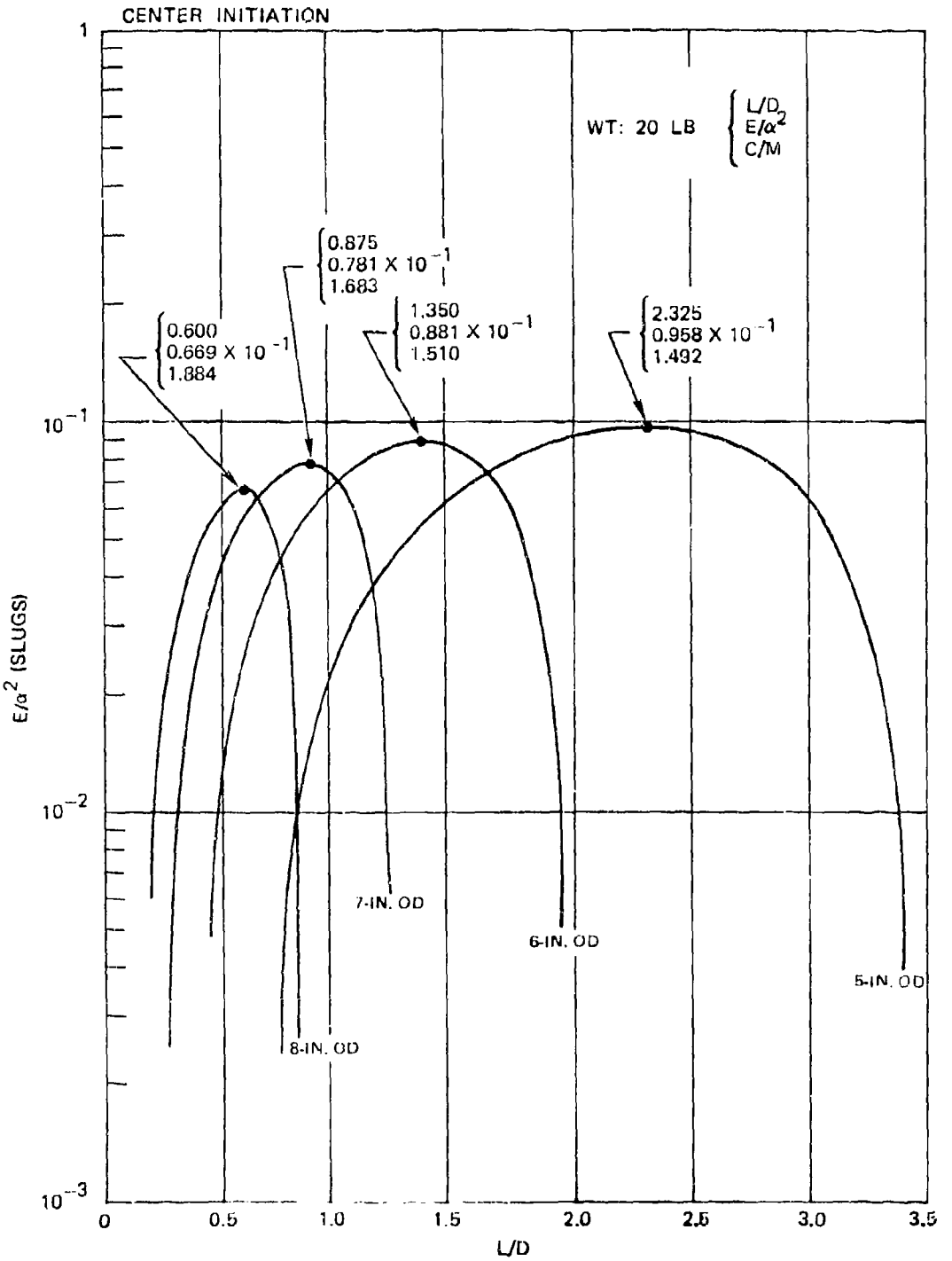

FIGURE 12. Fragment Initial Kinetic Energy Envelopes for Indicated Weight, Center Initiation.

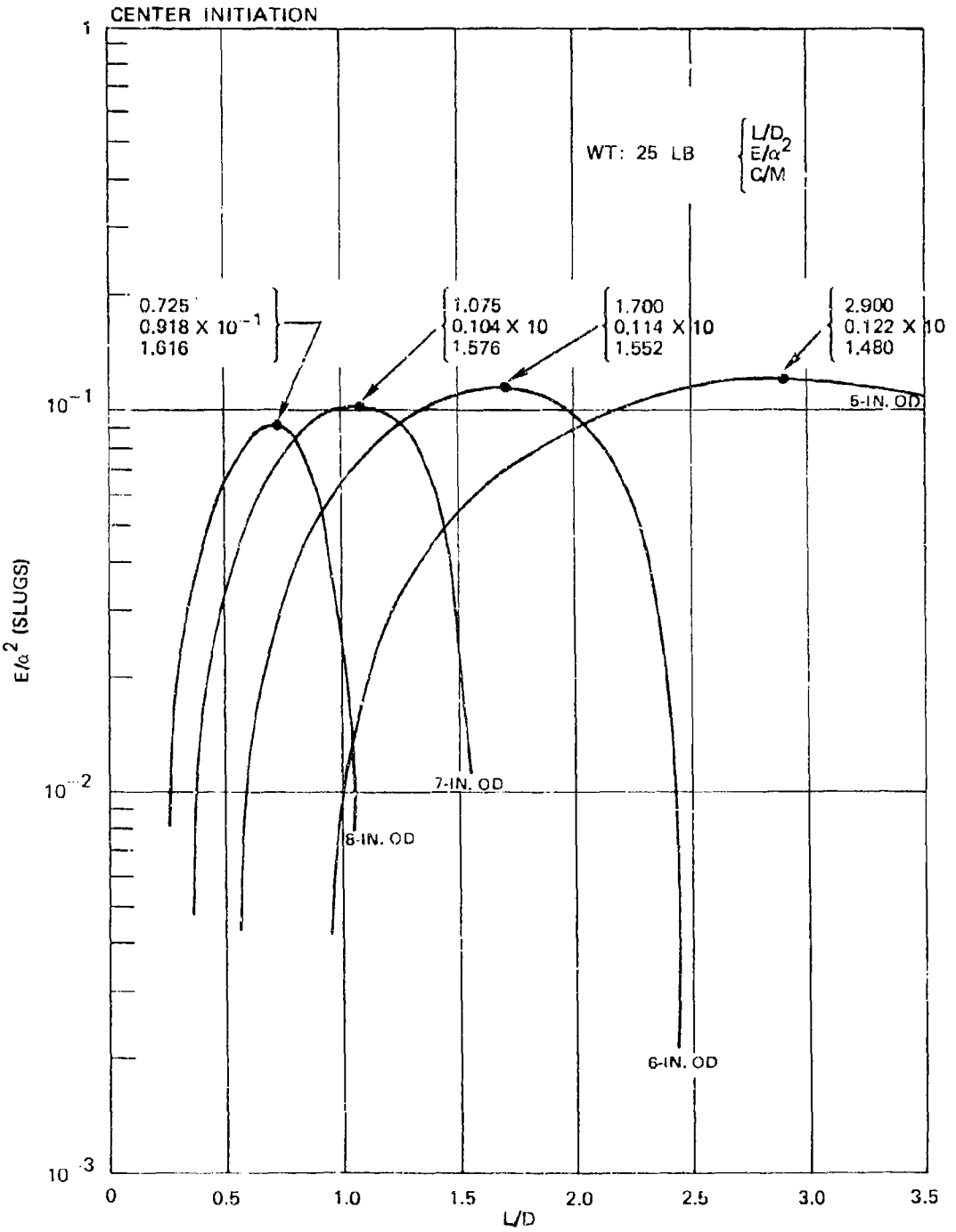

FIGURE 13. Fragment Initial Kinetic Energy Envelopes for Indicated Weight, Center Initiation.

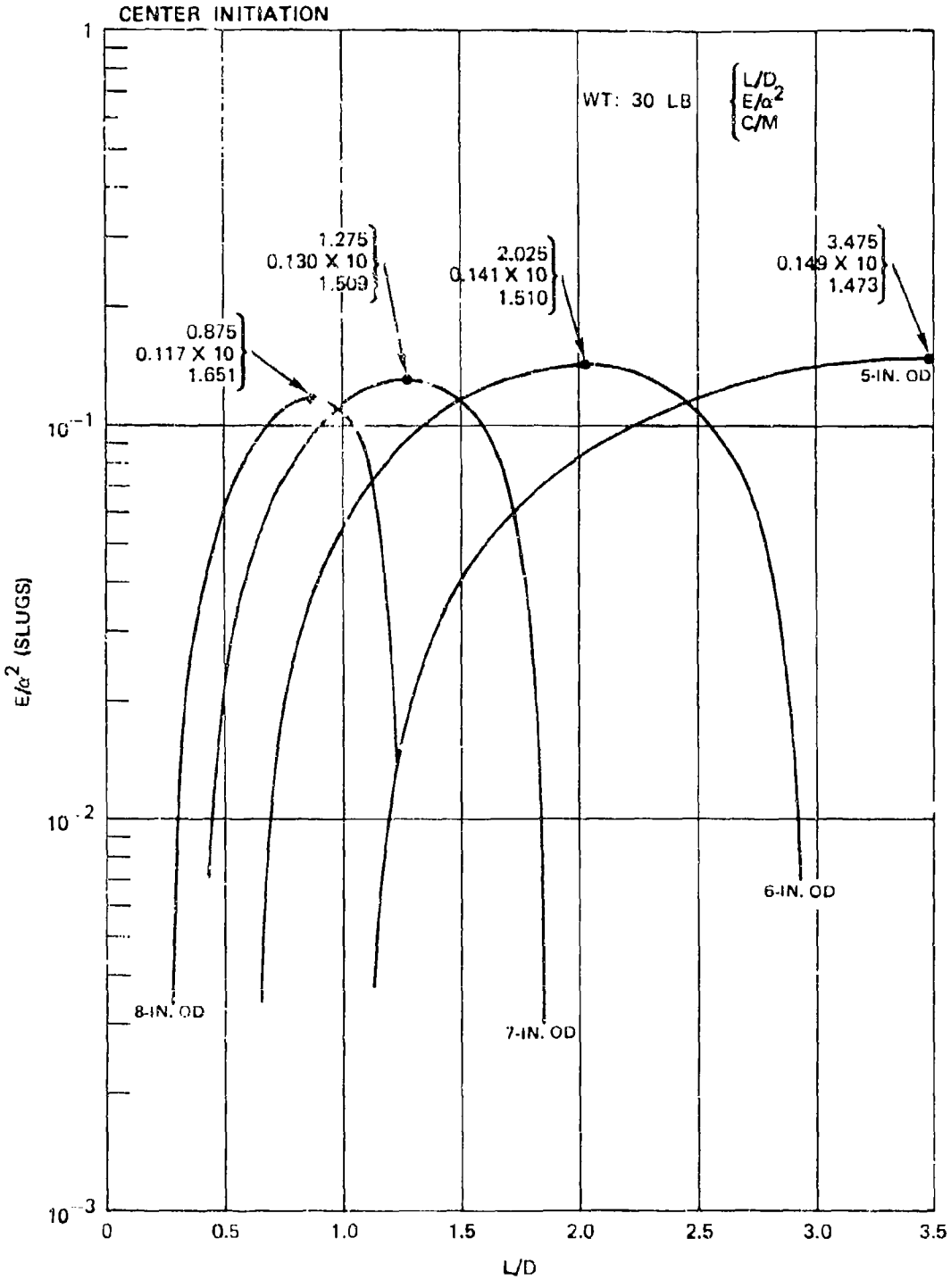

FIGURE 14. Fragment Initial Kinetic Energy Envelopes for Indicated Weight, Center Initiation.

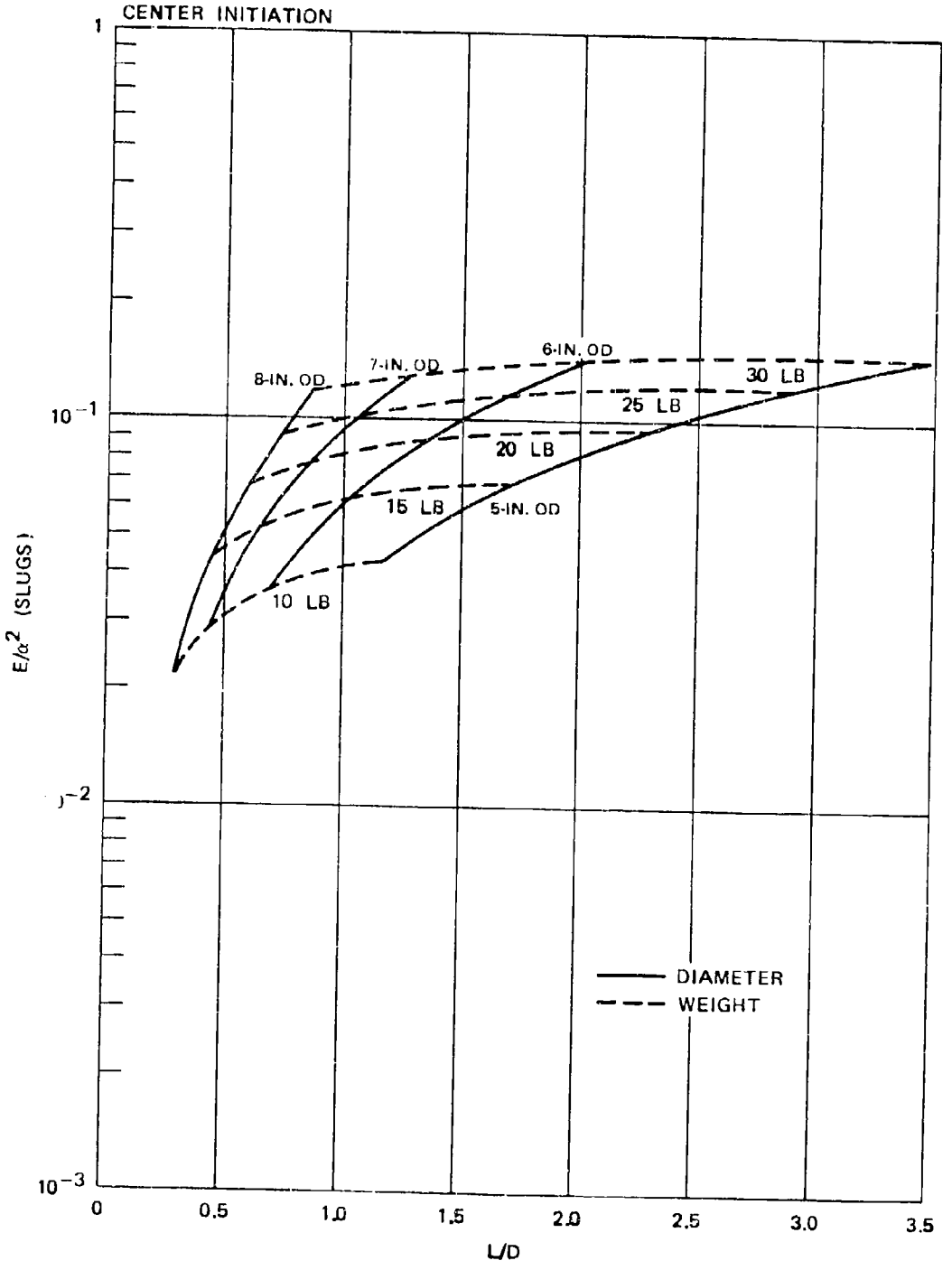

FIGURE 15. Maximum Initial Kinetic Energy Envelopes for Center Initiation as a Function of Weight and Diameter.

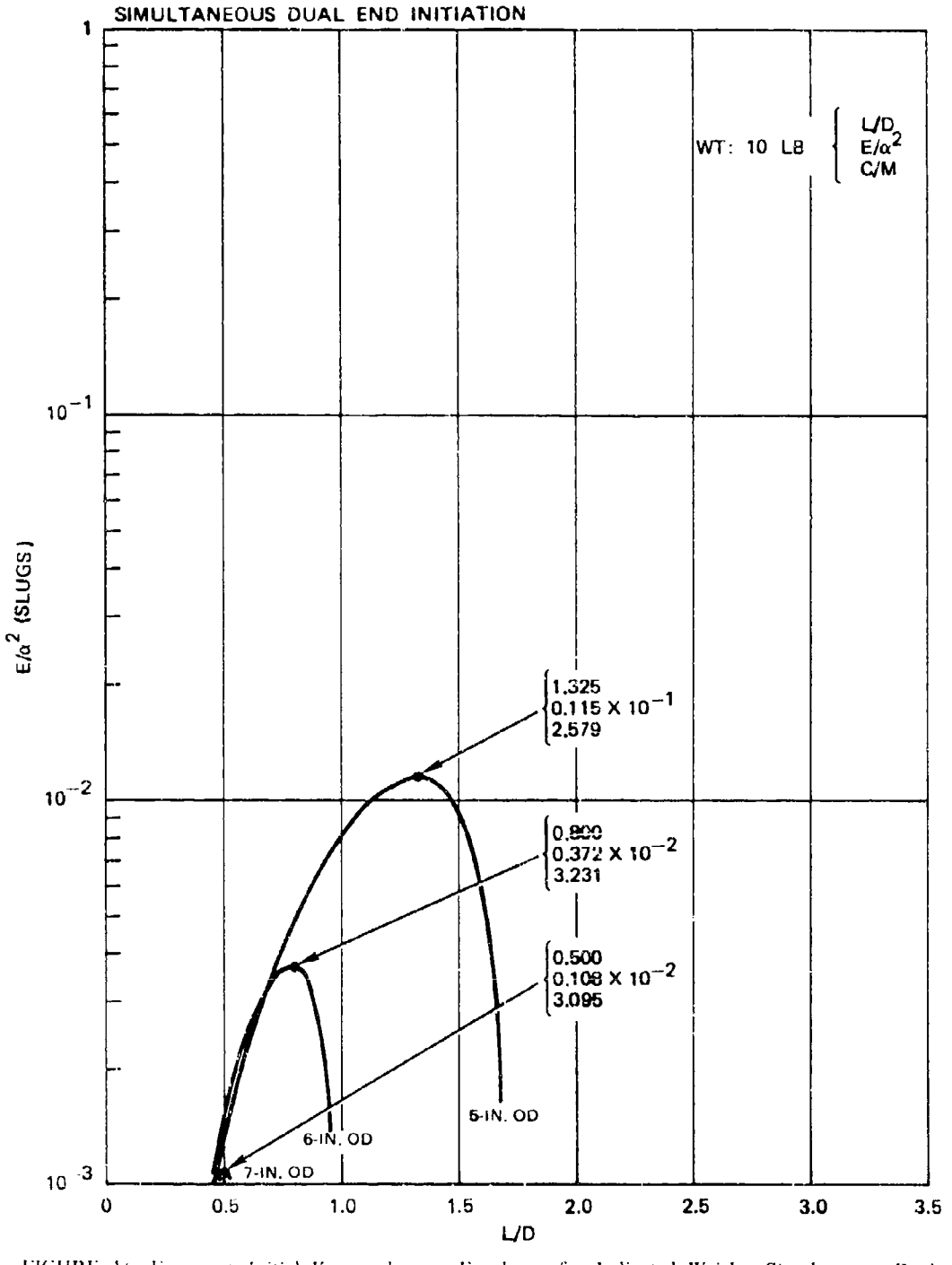

FIGURE 16. Fragment Initial Kinetic Energy Envelopes for Indicated Weight, Simultaneous Dual End Initiation.

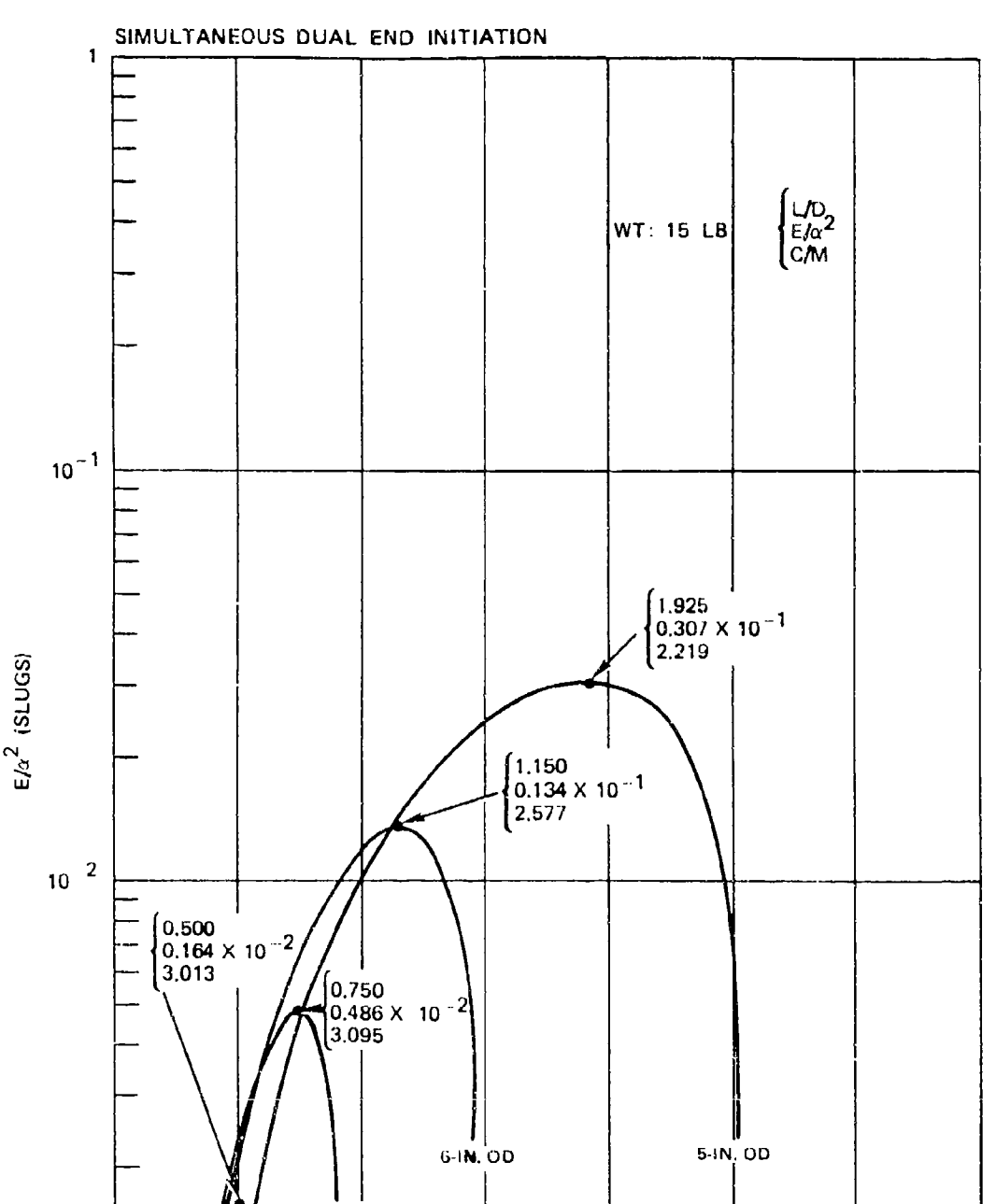

FIGURE 17. Fragment Initial Kinetic Energy Envelopes for Indicated Weight, Simultaneous Dual End Initiation.

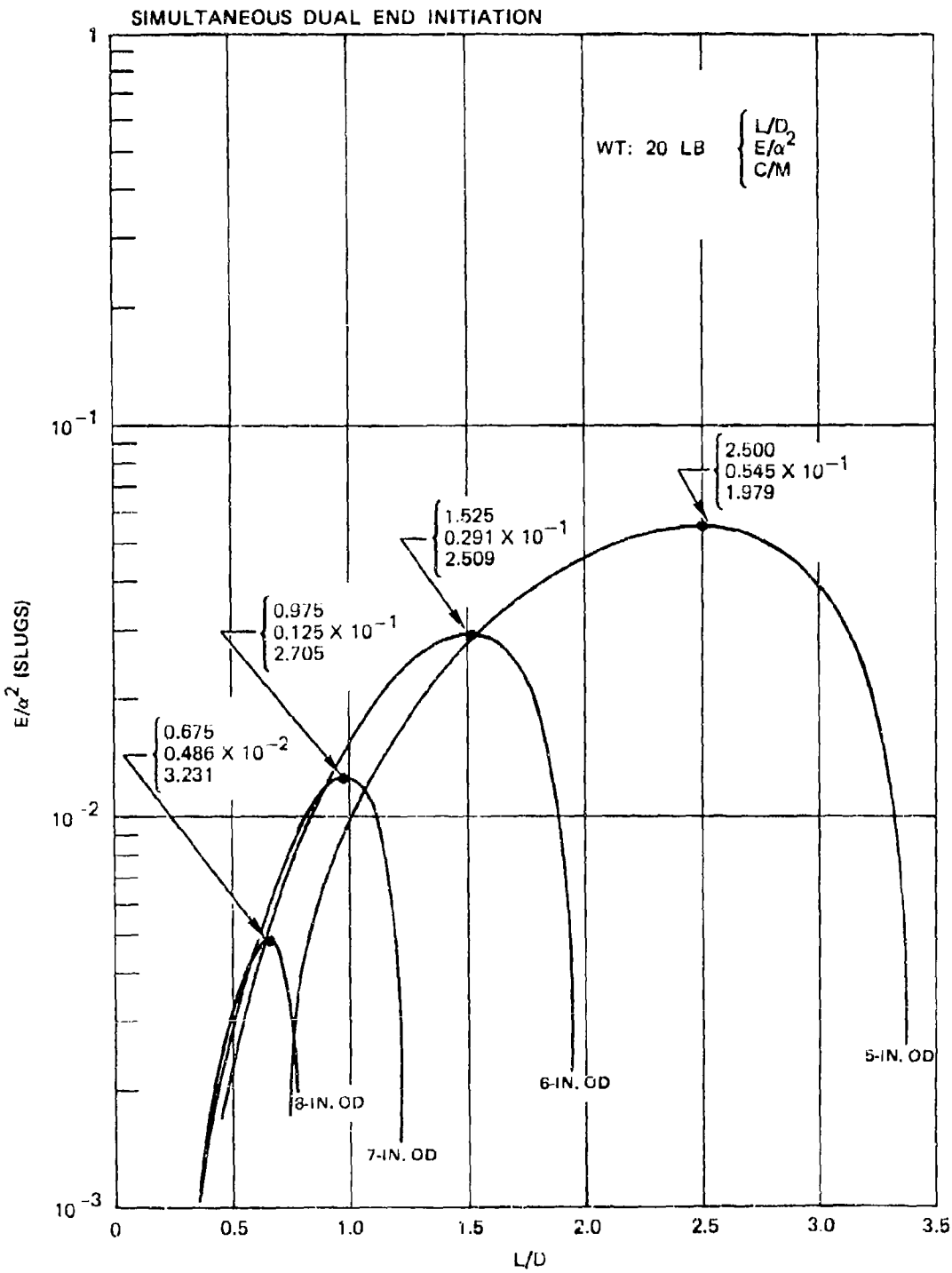

FIGURE 18. Fragment Initial Kinetic Energy Envelopes for Indicated Weight, Simultaneous Dual End Initiation.

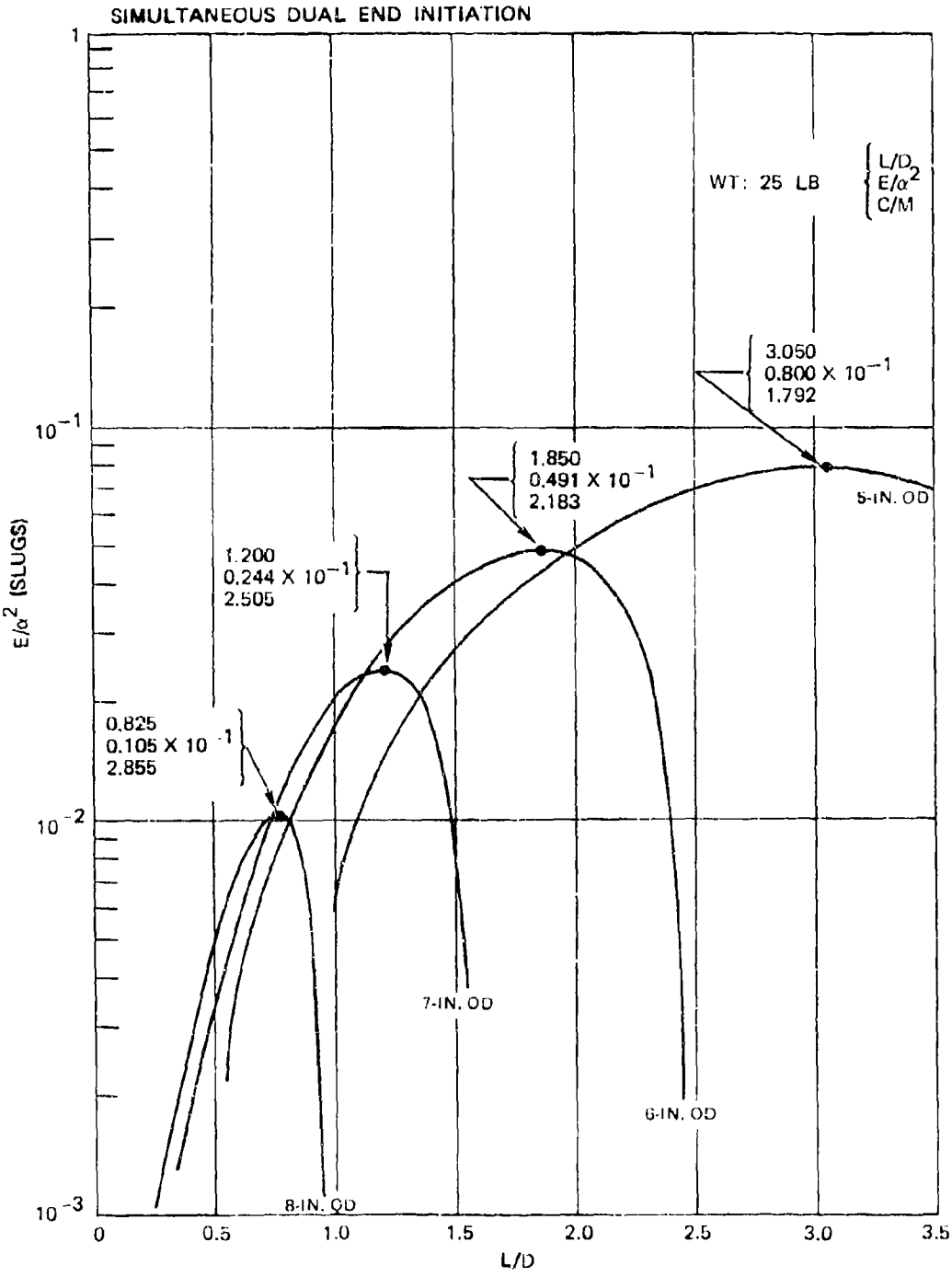

FIGURE 19. Fragment Initial Kinetic Energy Envelopes for Indicated Weight, Simultaneous Dual End Initiation.

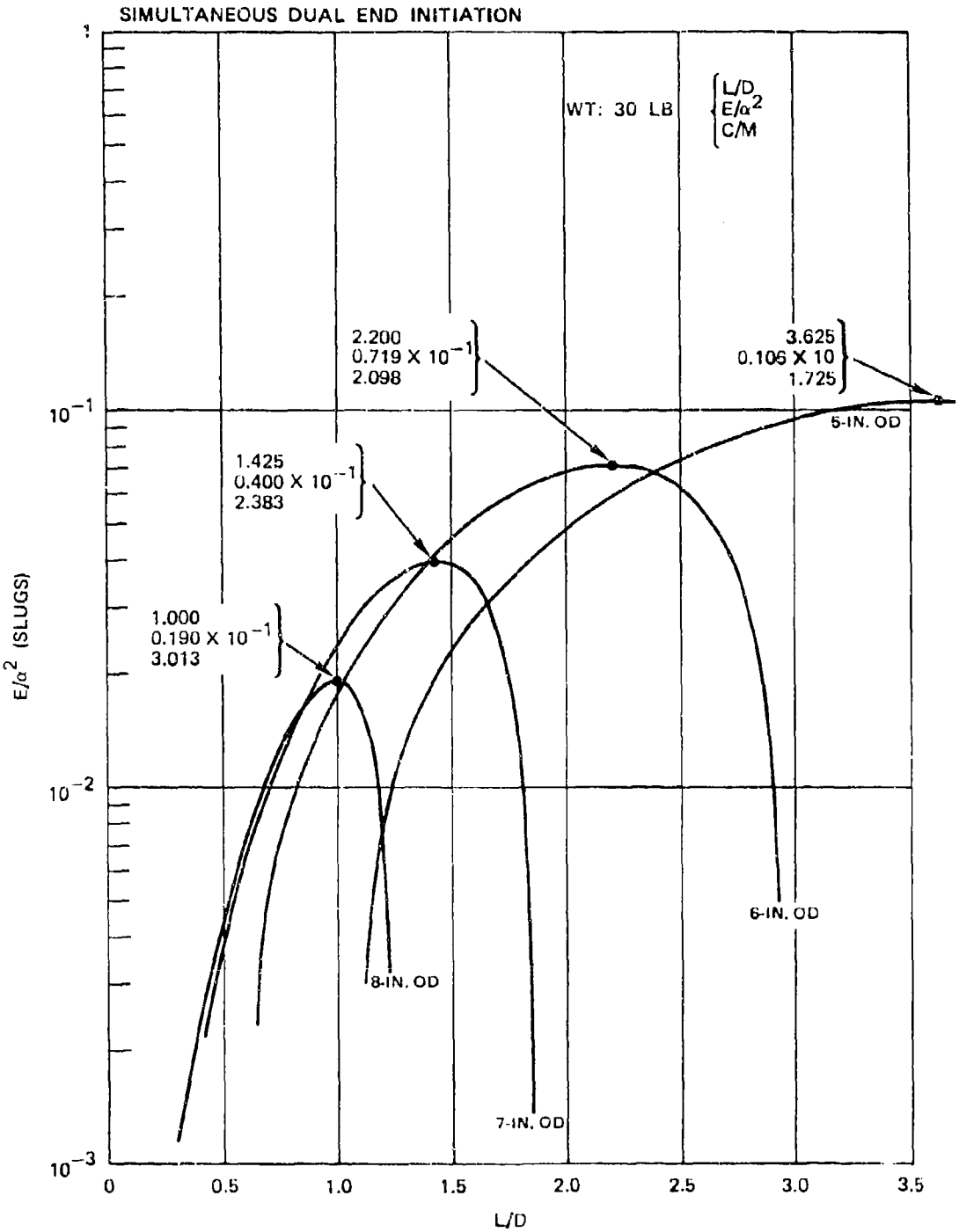

FIGURE 20. Fragment Initial Kinetic Energy Envelopes for Indicated Weight, Simultaneous Dual End Initiation.

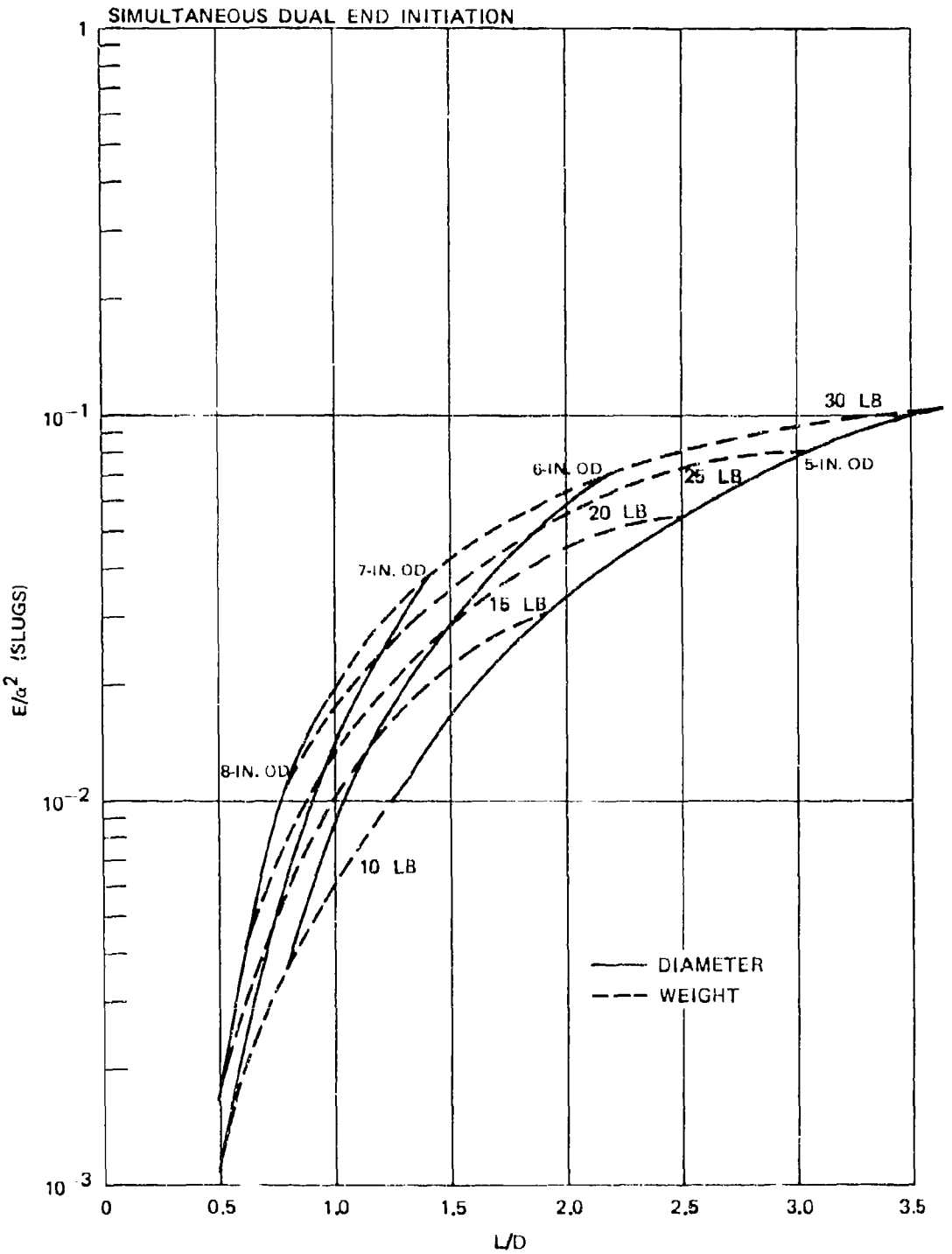

FIGURE 21. Maximum Initial Kinetic Energy Envelopes for Simultaneous Dual End Initiation as a Function of Weight and Diameter.

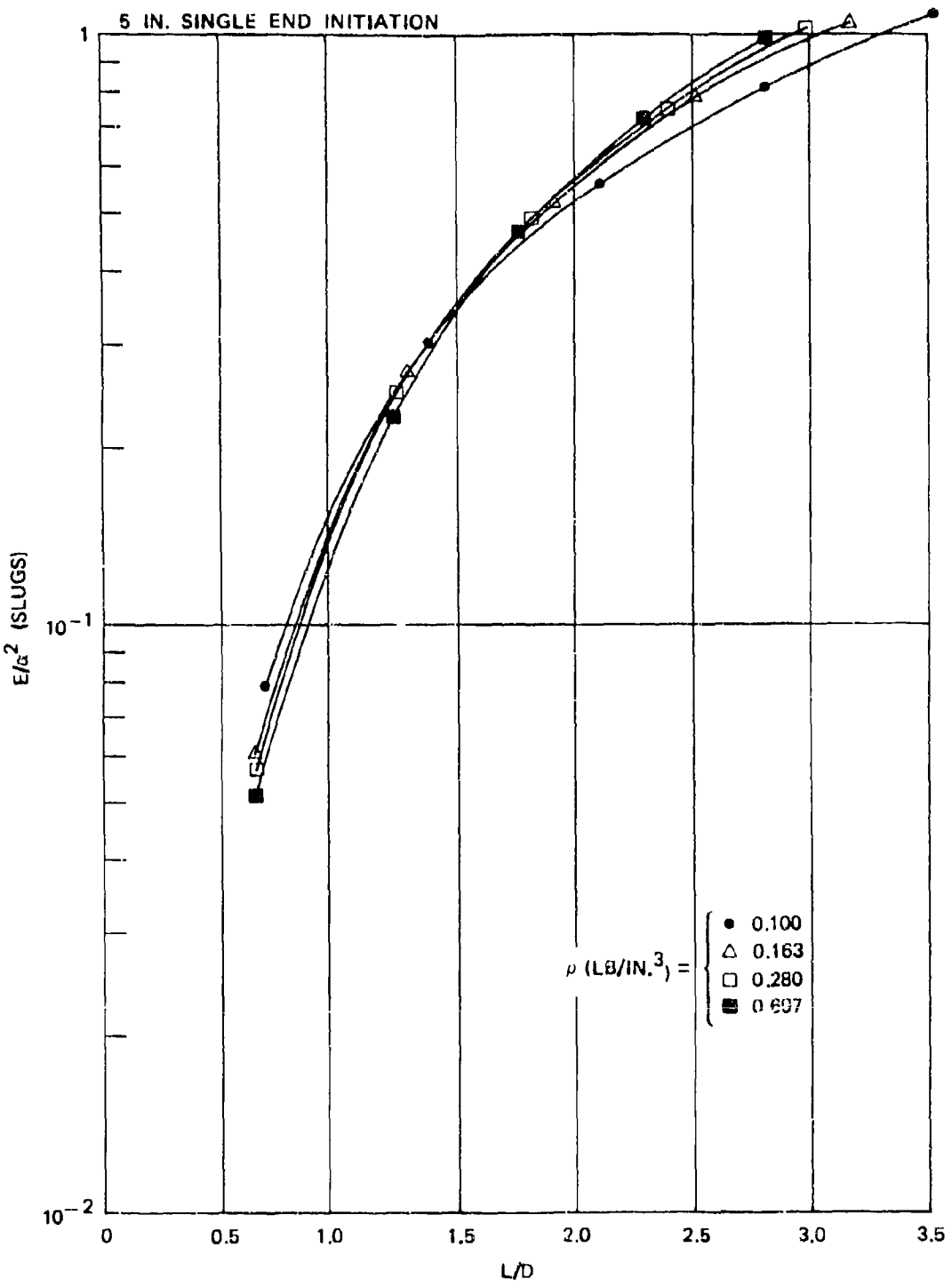

FIGURE 22. Effect of Fragment Density on Maximum Initial Kinetic Energy Envelopes as a Function of Diameter and L/D.

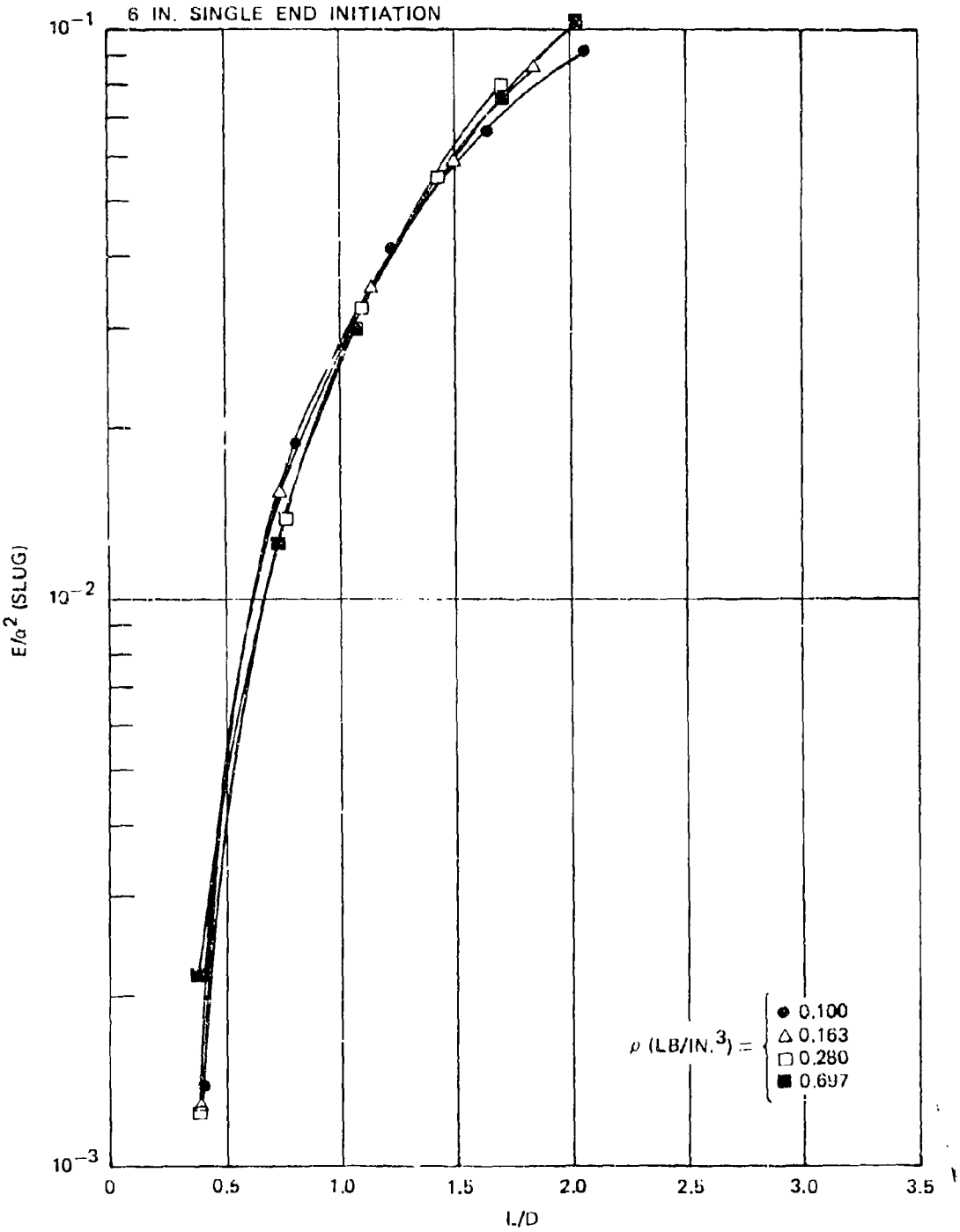

FIGURE 23. Effect of Fragment Density on Maximum Initial Kinetic Energy Envelopes as a Function of Diameter and L/D.

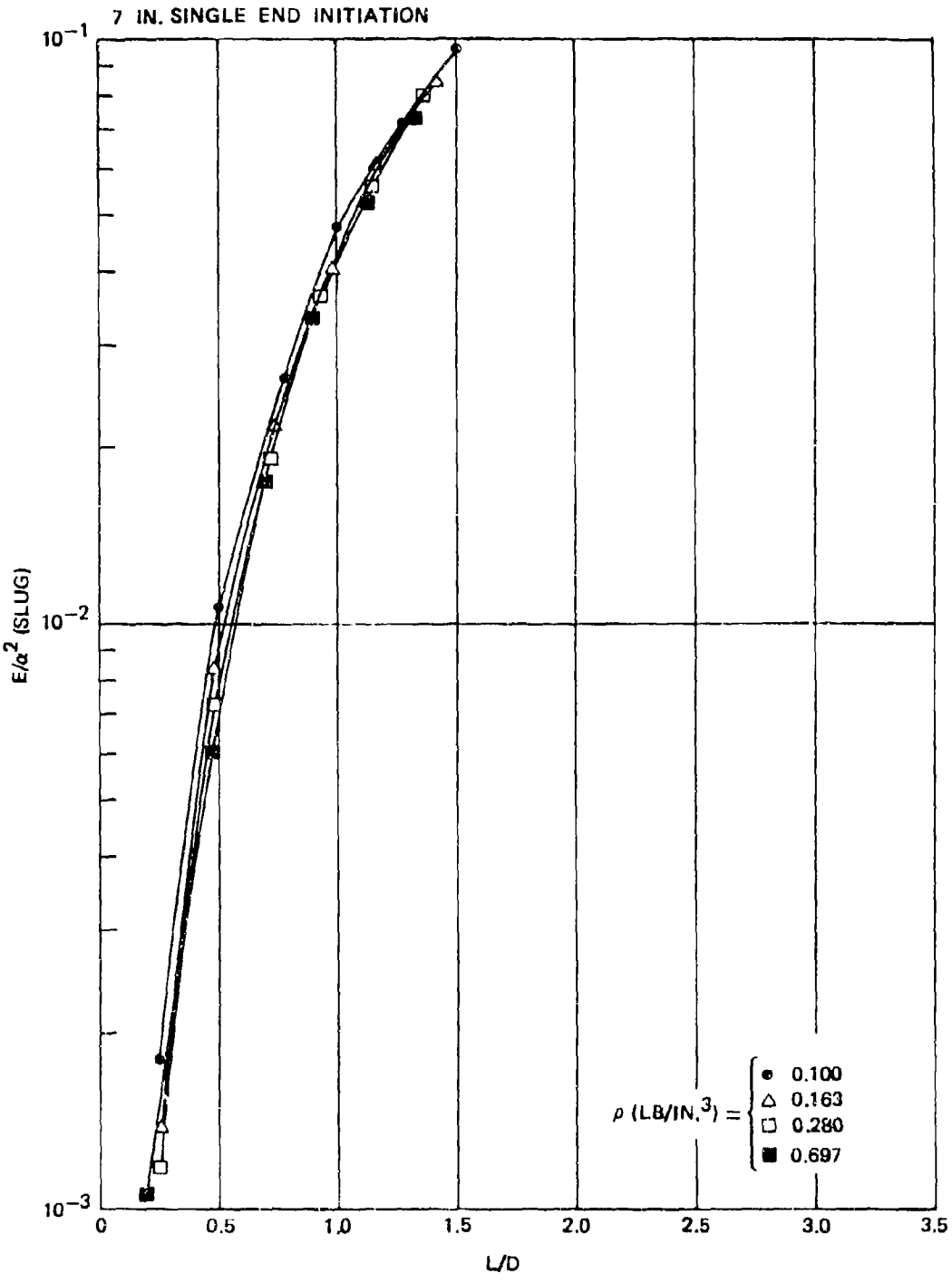

FIGURE 24. Effect of Fragment Density on Maximum Initial Kinetic Energy Envelopes as a Function of Diameter and L/D.

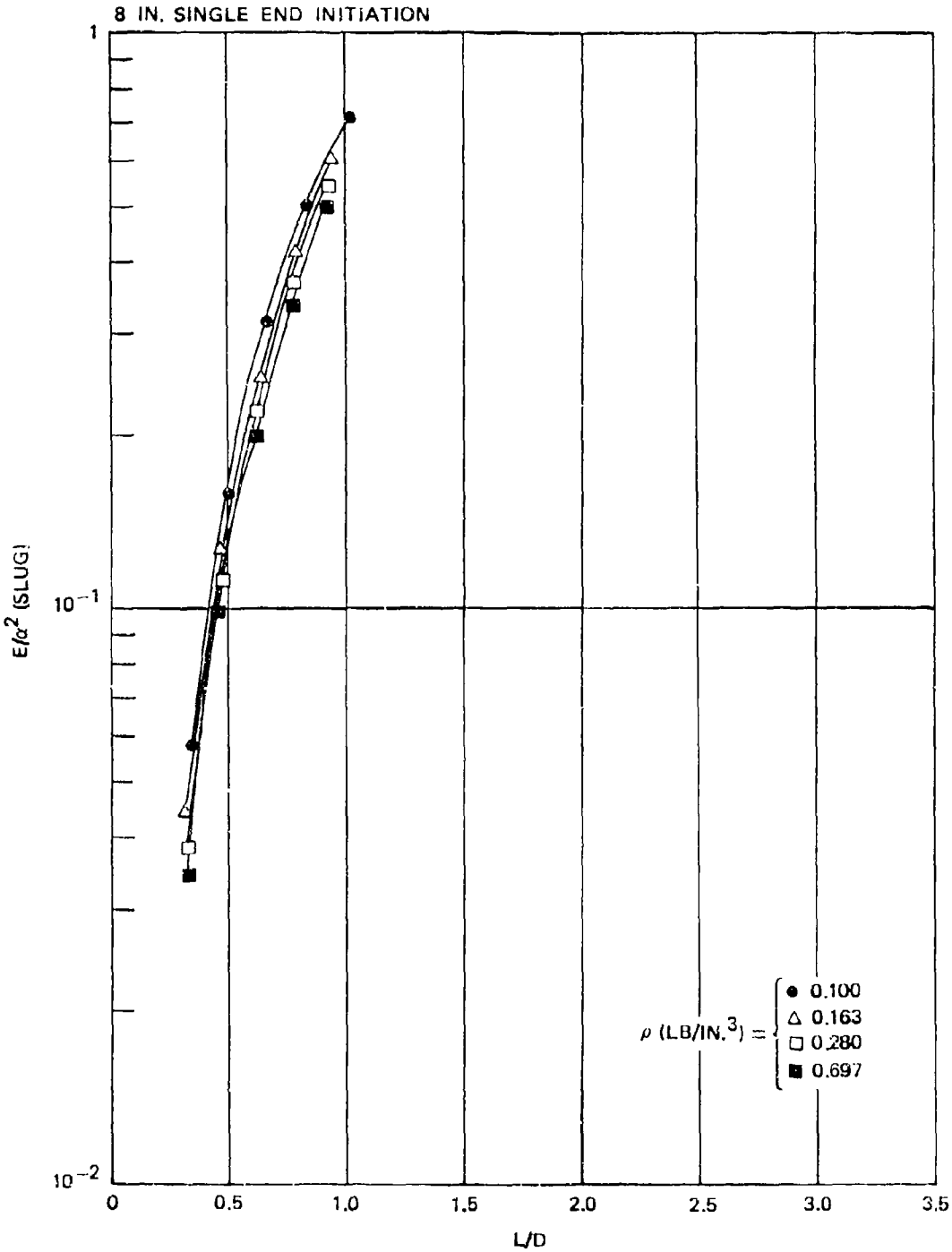

FIGURE 25. Effect of Fragment Density on Maximum Initial Kinetic Energy Envelopes as a Function of Diameter and L/D.

INITIAL DISTRIBUTION

14 Naval Air Systems Command
- AIR-03P2 (1)
- AIR-09E3A (1)
- AIR-350 (2)
- AIR-5108 (1)
- AIR-5108B (1)
- AIR-5109B1 (1)
- AIR-5109C2 (1)
- AIR-532 (1)
- AIR-5323 (1)
- AIR-5324 (1)
- AIR-53242 (1)
- AIR-954 (2)

6 Chief of Naval Operations
- OP-03EG (1)
- OP-342 (1)
- OP-506 (1)
- OP-506F (1)
- OP-982 (1)
- OP-982E42 (1)

7 Naval Sea Systems Command
- SEA-0333 (1)
- SEA-0411 (1)
- SEA-09G32 (2)
- SEA-6543 (1)
- SEA-6543C (1)
- PMS-40622 (1)

1 Chief of Naval Research, Arlington (ONR-461)
1 Commandant of the Marine Corps (Code AAW-1)
2 Marine Corps Development and Education Command, Quantico
- Mobility Support Division, Major Thorp (1)
- War Games Division, Marine Corps Landing Force Development Center (1)

1 Air Test and Evaluation Squadron 5
1 Naval Ammunition Depot, Earle
1 Naval Ammunition Depot, Hawthorne (Code 05, Robert Dempsey)
1 Naval Coastal Systems Laboratory, Panama City (Code 772)
1 Naval Explosive Ordnance Disposal Facility, Indian Head
1 Naval Intelligence Support Center (Code OOXA, Cdr. Jack Darnell)
1 Naval Ordnance Station, Indian Head (Technical Library)
1 Naval School Explosive Ordnance Disposal, Naval Ordnance Station, Indian Head
1 Naval Special Warfare Group, Atlantic (RDT&E)
1 Naval Special Warfare Group, Pacific (RDT&E)

13 Naval Surface Weapons Center, White Oak
- Code 0431, G. Klamm (1)
- Code ESE, S. Mason (1)
- Code GWA (1)
- Code KM (1)
- Code NS (1)
- Code T (1)
- Code W (1)
- Code WR-12
  - L. Anderson (1)
  - M. Stosz (1)
- Code WER
- Code WR-13, N. L. Coleburn (1)
- Code WR-102, I. Kabik (1)
- Code WWB (1)
- Code XWF (1)

1 Naval Undersea Center, San Diego (Code 133)
1 Naval Weapons Station, Yorktown (Research and Development Division)
1 Naval Weapons Support Center, Crane
1 Navy Ships Parts Control Center, Mechanicsburg (Code AMb)
1 Nuclear Weapons Training Center, Atlantic
1 Nuclear Weapons Training Center, Pacific (Conventional Weapons Employment Course)
2 Pacific Missile Test Center, Point Mugu
- Code N322 (1)
- Code N1124 (1)

1 Naval Intelligence Support Center Liaison Officer (LNN)
4 Army Armament Command, Rock Island (AMSAR-SF)
1 Army Combat Development Command, Infantry Agency, Fort Benning
1 Army Materiel Command (AMCRD-J)
1 Army Ballistics Research Laboratory, Aberdeen Proving Ground (AMSRD-BTL, C. Kingery)
12 Picatinny Arsenal
- SARPA-AD-D-W (2)
- SMD, Concepts Branch (4)
- SMUPA-D (3)
- SMUPA-DM2 (1)
- SMUPA-EP, Dr. Norman Slagg (1)
- SMUPA-VE-5 (1)

1 Headquarters, U.S. Air Force (AFCSAM-I)
1 Air Force Logistics Command, Wright-Patterson Air Force Base (MCMTM)
4 Air Force Systems Command, Andrews Air Force Base
- DL (1)
- DLPI (1)
- DLW (1)
- SDW (1)